

RECEIVED: June 6, 2018

REVISED: July 20, 2018

ACCEPTED: August 5, 2018

PUBLISHED: August 10, 2018

Search for pair production of heavy vector-like quarks decaying into high- p_T W bosons and top quarks in the lepton-plus-jets final state in pp collisions at $\sqrt{s} = 13$ TeV with the ATLAS detector



The ATLAS collaboration

E-mail: atlas.publications@cern.ch

ABSTRACT: A search is presented for the pair production of heavy vector-like B quarks, primarily targeting B quark decays into a W boson and a top quark. The search is based on 36.1 fb^{-1} of pp collisions at $\sqrt{s} = 13$ TeV recorded in 2015 and 2016 with the ATLAS detector at the CERN Large Hadron Collider. Data are analysed in the lepton-plus-jets final state, characterised by a high-transverse-momentum isolated electron or muon, large missing transverse momentum, and multiple jets, of which at least one is b -tagged. No significant deviation from the Standard Model expectation is observed. The 95% confidence level lower limit on the B mass is 1350 GeV assuming a 100% branching ratio to Wt . In the SU(2) singlet scenario, the lower mass limit is 1170 GeV. The 100% branching ratio limits are found to be also applicable to heavy vector-like X production, with charge +5/3, that decay into Wt . This search is also sensitive to a heavy vector-like B quark decaying into other final states (Zb and Hb) and thus mass limits on B production are set as a function of the decay branching ratios.

KEYWORDS: Exotics, Hadron-Hadron scattering (experiments), vector-like quarks

ARXIV EPRINT: [1806.01762](https://arxiv.org/abs/1806.01762)

Contents

1	Introduction	1
2	ATLAS detector	3
3	Data and simulation	4
4	Analysis object selection	5
5	Analysis strategy	7
5.1	Event preselection	7
5.2	Classification of event topologies	8
5.2.1	RECOISR definition	8
5.2.2	BDTSR definition	10
5.3	Multi-jet background estimation	11
6	Systematic uncertainties	12
6.1	Luminosity and normalisation uncertainties	12
6.2	Detector-related uncertainties	12
6.3	Generator modelling uncertainties	13
7	Results	13
7.1	Statistical interpretation	13
7.2	Likelihood fit results	14
7.3	Limits on VLQ pair production	15
8	Conclusions	18
The ATLAS collaboration		24

1 Introduction

The discovery of the Higgs boson by the ATLAS and CMS collaborations is a major milestone in high-energy physics [1, 2]. However, the underlying nature of electroweak symmetry breaking remains unknown. Naturalness arguments [3] require that, to avoid fine-tuning, quadratic divergences arising from radiative corrections to the Higgs boson mass are cancelled out by one or more new particles. Several such mechanisms have been proposed in theories beyond the Standard Model. In supersymmetry, the cancellation comes from assigning superpartners to the Standard Model (SM) bosons and fermions. Alternatively, Little Higgs [4, 5] and Composite Higgs [6, 7] models introduce a spontaneously

broken global symmetry, with the Higgs boson emerging as a pseudo Nambu–Goldstone boson [8]. These latter models predict the existence of vector-like quarks (VLQs), defined as colour-triplet spin-1/2 fermions whose left- and right-handed chiral components have the same transformation properties under the weak-isospin SU(2) gauge group [9, 10]. Depending on the model, vector-like quarks are produced in SU(2) singlets, doublets, or triplets of flavours T , B , Y or X , in which the first two have the same charge as the SM top quark and b -quark while the vector-like Y and X quarks have charge¹ $-4/3$ and $+5/3$, respectively. In addition, in these models, VLQs are expected to couple preferentially to third-generation quarks [9, 11] and can have flavour-changing neutral-current decays at leading order in addition to the charged-current decays characteristic of chiral quarks. As a result, an up-type T quark can decay not only into a W boson and a b -quark, but also into a Z or Higgs boson and a top quark ($T \rightarrow Wb$, Zt , and Ht). Similarly, a down-type B quark can decay into a Z or Higgs boson and a b -quark, in addition to decaying into a W boson and a top quark ($B \rightarrow Wt$, Zb , and Hb). For each type, the sum of the three branching fractions is assumed to be 1, i.e. other decays are not considered. Due to their charge, vector-like Y quarks can only decay into Wb while vector-like X quarks must decay into Wt . To be consistent with the results from precision electroweak measurements, the mass-splitting between VLQs belonging to the same SU(2) multiplet is required to be small, but no requirement is placed on which member of the doublet is heavier [12]. Cascade decays such as $T \rightarrow WB \rightarrow WWt$ are thus assumed to be kinematically forbidden. Decays of VLQs into final states with first- and second-generation quarks, although not favoured, are not excluded by precision electroweak or flavour measurements [13, 14].

This search targets the $B\bar{B}$ pair-production with the subsequent decay mode $B \rightarrow Wt$ using the pp collision data collected at the Large Hadron Collider (LHC) in 2015 and 2016 at a centre-of-mass energy of 13 TeV, although it is also sensitive to a wide range of branching ratios to the other two decay modes as well as to production of vector-like X quarks. Contrary to single production the $B\bar{B}$ pair-production cross section depends only on the B quark mass. An example of a leading-order production diagram is shown in figure 1. Previous searches in this decay mode by the ATLAS and CMS collaborations did not observe a significant deviation from the SM predictions. Those searches excluded VLQ masses below 740 GeV for any combination of branching ratios and below 1020 GeV for the assumption of $\mathcal{B}(B \rightarrow Wt) = 1$ [15, 16]. A recent search by the ATLAS Collaboration at $\sqrt{s} = 13$ TeV, primarily targeting the T quark decaying into Wb , was also found to be sensitive to B and X quarks decaying into Wt . The results included interpretations which provide a 95% confidence-level observed (expected) lower limit on the B quark mass at 1250 (1150) GeV assuming a 100% branching ratio to Wt ; in the SU(2) singlet scenario, the limit is 1080 (980) GeV [17]. In this context, the event selection for this new search is optimised for high-mass $B\bar{B}$ production with subsequent decay into two high- p_T W bosons and two top quarks, where one of the four W bosons decays leptonically and the others decay hadronically. To suppress the SM background, boosted-jet reconstruction techniques [18, 19] are used to improve the identification of hadronically decaying high- p_T

¹All electric charges are quoted in units of e .

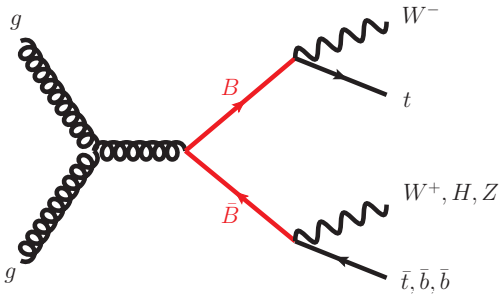


Figure 1. Example of a leading-order $B\bar{B}$ production diagram in the targeted Wt decay mode.

W bosons and top quarks. The decay products of a hadronically decaying high-momentum W boson are likely to be contained within a single large-radius jet. The two signal regions used in this search are based on the number of reconstructed large-radius jets. The first signal region aims to reconstruct the $B\bar{B}$ system using the mass of the purely hadronically decaying B candidate to discriminate between SM and VLQ events. The second, more inclusive, signal region uses a Boosted Decision Tree (BDT) to discriminate between SM and VLQ events.

Finally, a profile likelihood fit is used to test for the presence of a VLQ signal as a function of the B quark mass and the decay branching ratios. The results are found to be equally applicable to either singlet or doublet weak-isospin configurations as well as to the decays of X quarks.

2 ATLAS detector

The ATLAS detector [20] at the LHC is a multipurpose particle detector with a forward-backward symmetric cylindrical geometry that covers nearly the entire solid angle around the collision point. It consists of an inner detector surrounded by a thin superconducting solenoid providing a 2 T axial magnetic field, electromagnetic and hadronic calorimeters, and a muon spectrometer. The inner detector covers the pseudorapidity range² $|\eta| < 2.5$. It consists of a silicon pixel detector, including the insertable B-layer installed after Run 1 of the LHC [21, 22], and a silicon microstrip detector surrounding the pixel detector, followed by a transition radiation straw-tube tracker. Lead/liquid-argon sampling calorimeters provide electromagnetic energy measurements with high granularity and a hadronic (steel/scintillator-tile) calorimeter covers the central pseudorapidity range ($|\eta| < 1.7$). The endcap and forward regions are instrumented with liquid-argon calorimeters for both the electromagnetic and hadronic energy measurements up to $|\eta| = 4.9$. The outer part of the detector consists of a muon spectrometer with high-precision tracking chambers for

²The ATLAS Collaboration uses a right-handed coordinate system with its origin at the nominal interaction point (IP) in the centre of the detector and the z -axis along the beam pipe. The x -axis points from the IP to the centre of the LHC ring, and the y -axis points upwards. Cylindrical coordinates (r, ϕ) are used in the transverse plane, ϕ being the azimuthal angle around the z -axis. The pseudorapidity is defined in terms of the polar angle θ as $\eta = -\ln(\tan(\theta/2))$. Angular distance is measured in units of $\Delta R \equiv \sqrt{(\Delta\eta)^2 + (\Delta\phi)^2}$.

coverage up to $|\eta| = 2.7$, fast detectors for triggering over $|\eta| < 2.4$, and three large superconducting toroid magnets with eight coils each. The ATLAS detector has a two-level trigger system to select events for offline analysis [23].

3 Data and simulation

Data are only used if all ATLAS detector subsystems were operational. This search utilises a data set corresponding to 36.1 fb^{-1} of integrated luminosity from pp collisions at $\sqrt{s} = 13 \text{ TeV}$ collected by the ATLAS experiment, with 3.2 fb^{-1} collected in 2015 and 32.9 fb^{-1} collected in 2016.

In all simulated events used in this search, the top quark and Higgs boson masses were set to 172.5 GeV and 125 GeV, respectively. Simulated $B\bar{B}$ signal events were generated with the leading-order (LO) generator PROTON v2.2 [24] using the NNPDF2.3 [25] LO parton distribution function (PDF) set and a set of tuned parameters called the A14 tune [26] and were passed to PYTHIA 8.186 [27] for the underlying-event description, parton showering, and fragmentation. The samples were generated for an SU(2) singlet B VLQ, but with equal branching ratios of the B quark to each final state. To check the dependence of the results on the weak-isospin of the VLQ, one sample was also generated using the SU(2) (T_B) doublet model including only the B contributions. The signal samples are normalised to pair-production cross-sections computed using TOP++ v2.0 [28], including next-to-next-to-leading-order (NNLO) quantum chromodynamics (QCD) corrections and soft-gluon resummation to next-to-next-to-leading-logarithm (NNLL) accuracy [29–34], and using the MSTW 2008 NNLO PDF set [35]. Their cross-sections vary from $3.38 \pm 0.25 \text{ pb}$ ($m_B = 500 \text{ GeV}$) to $0.13 \pm 0.02 \text{ fb}$ ($m_B = 2000 \text{ GeV}$). Theoretical uncertainties are evaluated from variations of the factorisation and renormalisation scales, as well as from uncertainties in the PDFs and α_S . The latter two represent the largest contribution to the overall theoretical uncertainty in the signal cross-sections and are calculated using the PDF4LHC [36] prescription with the MSTW 2008 68% CL NNLO, CT10 NNLO [37, 38] and NNPDF2.3 5f FFN PDF sets [25]. Two benchmark signal scenarios are considered, along with a full scan of the branching-ratio plane. The first benchmark corresponds to a B quark that decays 100% into Wt and the second corresponds to the SU(2) singlet B quark scenario, which predicts branching ratios of $\sim 50\%$, $\sim 25\%$, $\sim 25\%$ to Wt , Zb and Hb , respectively [12].

The main SM backgrounds that are studied using simulated samples are $t\bar{t}$, $W + \text{jets}$, $Z + \text{jets}$, diboson, single top quark, and $t\bar{t}V$ ($V = W, Z$). The nominal $t\bar{t}$ Monte Carlo sample was generated with POWHEG-BOX v2 [39] interfaced with PYTHIA 8.2 [40] for the parton shower and hadronisation, using the A14 tune and the NNPDF2.3 LO PDF set, setting the next-to-leading-order (NLO) radiation factor, h_{damp} , to 1.5 times the mass of the top quark, m_{top} . To estimate $t\bar{t}$ modelling uncertainties, described in section 6.3, additional samples were generated using POWHEG-BOX v2 interfaced with HERWIG 7 [41], and MADGRAPH5_aMC@NLO 2.1.1 [42] interfaced with PYTHIA 8.2. In addition, samples with POWHEG-BOX v2 interfaced with PYTHIA 8.2 were generated with the factorisation and renormalisation scales varied by factors of 2 and 0.5, as well as with h_{damp} varied

between $1.5 \times m_{\text{top}}$ and $3 \times m_{\text{top}}$. The $t\bar{t}$ samples are normalised to the NNLO cross-section, including NNLO QCD corrections and soft-gluon resummation to NNLL accuracy, as performed for the signal samples.

Single top quark production (called ‘single top’ in the following) in the s -channel and in Wt final states was also generated with POWHEG-Box v2 interfaced with PYTHIA 6.428 [43], while single top production in the t -channel was generated with POWHEG-Box v1 interfaced with PYTHIA 6.428 for the parton shower and hadronisation. Single-top samples were generated using the PERUGIA2012 tune [44] and the CT10 PDF set [38]. The diagram removal method was used to remove the overlap between NLO Wt production and LO $t\bar{t}$ production [45]. The single-top cross-sections for the t - and s -channels are normalised to their NLO predictions using HATHOR v2.1 [46, 47], while for the Wt final states the cross-section is normalised to its NLO+NNLL prediction [48]. For $W + \text{jets}$, $Z + \text{jets}$, and diboson (WW , WZ , ZZ) samples, the SHERPA 2.2.1 generator [49] was used with the CT10 PDF set. The $W + \text{jets}$ and $Z + \text{jets}$ production samples are normalised to the NNLO cross-sections [50–52]. For diboson production, the generator cross-sections (already at NLO) are used for the sample normalisation. The $t\bar{t}V$ background is modelled using samples produced with MADGRAPH5_aMC@NLO 2.1.1 interfaced with PYTHIA 8.186, using the A14 tune and the NNPDF2.3 LO PDF set. The $t\bar{t}+V$ samples are normalised to their respective NLO cross-sections [42].

All simulated events, except those from SHERPA, use EVTGEN v1.2.0 [53] for the modelling of b -hadron decays. All simulated event samples for the nominal predictions were produced using the ATLAS simulation infrastructure [54], using the full GEANT 4 [55] simulation of the ATLAS detector. The alternative $t\bar{t}$ generator samples were processed with a fast simulation [56] of the ATLAS detector with parameterised showers in the calorimeters. Simulated events were then reconstructed with the same software as used for the data. Multiple overlaid pp collisions in the same or nearby bunch crossings (pile-up) were simulated at rates matching those in the data; they were modelled as low- p_T multi-jet production using the PYTHIA 8.186 generator and the A2 tune [57]. Additional corrections are applied to the simulated samples to correct for residual deviations of efficiencies and resolutions from those observed in the data.

4 Analysis object selection

Reconstructed objects are defined by combining information from different detector subsystems. This section outlines the criteria used to identify and select the reconstructed objects used in the analysis. Events are required to have at least one vertex candidate with at least two tracks with $p_T > 400$ MeV. The primary vertex is taken to be the vertex candidate with the largest sum of squared transverse momenta of all associated tracks.

To reconstruct jets, three-dimensional energy clusters in the calorimeter [58], assumed to represent massless particles coming from the primary vertex, are grouped together using the anti- k_t clustering algorithm [59–61] with a radius parameter of 0.4 (1.0) for small- R (large- R) jets. Small- R jets and large- R jets are clustered independently using the same inputs.

Small- R jets are calibrated using an energy- and η -dependent calibration scheme, with *in situ* corrections based on data [62], and are selected if they have $p_T > 25$ GeV and $|\eta| < 2.5$. A multivariate jet vertex tagger (JVT) selectively removes small- R jets below 60 GeV that are identified as having originated from pile-up collisions rather than the hard scatter [63]. Jets containing b -hadrons are identified via an algorithm that uses multivariate techniques to combine information from the impact parameters of displaced tracks as well as topological properties of secondary and tertiary decay vertices reconstructed within the jet [64, 65]. A jet is considered b -tagged if the value for the multivariate discriminant is above the threshold corresponding to an efficiency of 77% for tagging a jet containing b -hadrons. The corresponding light-jet rejection factor is ~ 130 and the charm-jet rejection factor is ~ 6 , as determined in simulated $t\bar{t}$ events [66].

Large- R jets are built using the energy clusters in the calorimeter and then trimmed [67] to mitigate the effects of contamination from pile-up and to improve background rejection. The jet energy and pseudorapidity are further calibrated to account for residual detector effects using energy- and pseudorapidity-dependent calibration factors derived from simulation. The k_t -based trimming algorithm reclusters the jet constituents into subjets with a more finely grained resolution with an R -parameter set to $R_{\text{sub}} = 0.2$. Subjets that contribute less than 5% to the p_T of the large- R jets are discarded. The properties (e.g. transverse momentum and invariant mass) of the jet are recalculated using only the constituents of the remaining subjets. Trimmed large- R jets are only considered if they have $p_T > 200$ GeV and $|\eta| < 2.0$. No dedicated overlap-removal procedure between large- R and small- R jets is performed. To identify large- R jets that are likely to have originated from the hadronic decay of W bosons (W_{had}), jet substructure information is exploited using both the ratio of the energy correlation functions $D_2^{\beta=1}$ [68, 69] and the combined jet mass [70]. The combined jet mass is constructed using a combination of the calorimeter-derived jet mass, based on calorimeter cell cluster constituents, and the track-assisted jet mass, where the calorimeter momentum is augmented by information from the tracks associated with the large- R jet. Selected large- R jets must pass both the substructure and mass requirements of the 50%-efficient W -tagging working point [18]. To reduce the contribution from the $t\bar{t}$ background, W_{had} candidates must not overlap any b -tagged small- R jets within $\Delta R < 0.75$.

Electrons are reconstructed from energy deposits in the electromagnetic calorimeter matched to inner detector tracks. Electron candidates are required to satisfy likelihood-based identification criteria [71] and must have $p_T^{\text{ele}} > 30$ GeV and $|\eta| < 2.47$. Electron candidates in the transition region between the barrel and endcap electromagnetic calorimeters, $1.37 < |\eta| < 1.52$, are excluded. A lepton isolation requirement is implemented by calculating the quantity $I_R = \sum_{\Delta R(\text{track,ele}) < R_{\text{cut}}} p_{\text{T}}^{\text{track}}$, where R_{cut} is the smaller of $10 \text{ GeV}/p_T^{\text{ele}}$ and 0.2, and the track associated with the lepton is excluded from the calculation. The electron must satisfy $I_R < 0.06 \cdot p_T^{\text{ele}}$. Additionally, electrons are required to have a track satisfying $|d_0|/\sigma_{d_0} < 5$ and $|z_0 \sin \theta| < 0.5 \text{ mm}$, where d_0 is the transverse impact parameter and z_0 is the $r\phi$ projection of the impact point onto the z -axis. An overlap-removal procedure prevents double-counting of energy between an electron and nearby jets by removing jets if the separation between the electron and jet is within $\Delta R < 0.2$ and removing electrons

if the separation is within $0.2 < \Delta R < 0.4$. Subsequently, a large- R jet is removed if the separation between the electron and the large- R jet is within $\Delta R = 1.0$.

Muons are reconstructed from inner detector tracks matched to muon spectrometer tracks or track segments [72]. Candidate muons are required to satisfy quality specifications based on information from the muon spectrometer and inner detector. Furthermore, muons are required to be isolated using the same criterion that is applied to electrons and their associated tracks must satisfy $|z_0 \sin \theta| < 0.5$ mm and $|d_0|/\sigma_{d_0} < 3$. Muons are selected if they have $p_T > 30$ GeV and $|\eta| < 2.5$. An overlap-removal procedure is also applied to muons and jets. If a muon and a jet with at least three tracks are separated by $\Delta R < \min(0.4, 0.04 + 10 \text{ GeV}/p_T^\mu)$ the muon is removed; if the jet has fewer than three tracks, the jet is removed.

For a given reconstructed event, the negative vector sum of the p_T of all reconstructed leptons and small- R jets is defined as the missing transverse momentum (\vec{E}_T^{miss}) [73]. An extra term is included to account for ‘soft’ energy from inner detector tracks that are not matched to any of the selected objects but are consistent with originating from the primary vertex.

5 Analysis strategy

This search targets the decay of high-mass pair-produced VLQs, $B\bar{B}$, where one B quark decays into Wt and the other decays into Wt , Zb or Hb . Since a recent search by ATLAS [17], primarily targeting the T quark decays into Wb , has been reinterpreted to exclude VLQs decaying into Wt at 95% confidence level (CL) for masses below 1250 GeV, this search focuses on the decays of high-mass VLQs. The final state consists of a high- p_T charged lepton and missing transverse momentum from the decay of one of the W bosons, high-momentum large- R jets from hadronically decaying boosted W bosons, and multiple b -tagged jets. The event preselection is described in section 5.1 and the classification of events into two non-overlapping signal regions follows in section 5.2. The multi-jet background is estimated using a data-driven technique discussed in section 5.3.

5.1 Event preselection

Events were recorded using a combination of single-electron or single-muon triggers with isolation requirements. In 2015, the lowest p_T threshold was 24 GeV; in 2016, it ranged from 24 to 26 GeV. Additional triggers without an isolation requirement were used to recover efficiency for leptons with $p_T > 60$ GeV. Events are required to have exactly one lepton candidate (electron or muon, N_{lep}) that must be geometrically matched to the triggering lepton. Signal events are expected to have a high jet multiplicity (N_{jets}), since they include up to two b -jets ($N_{b\text{-jets}}$) as well as jets from the hadronic decay of up to three W bosons. Therefore, at least four small- R jets are required, of which at least one must be b -tagged. At least one large- R jet candidate, $N_{\text{jets}}^{\text{large}}$, with no W -tagging requirement applied, is required and the E_T^{miss} is required to be greater than 60 GeV. Signal events are expected to have characteristic high values in S_T , defined by the scalar sum of E_T^{miss} and

	RECOSR	BDTSR
Leptons	$N_{\text{lep}} = 1$	
Small- R jets	$N_{\text{jets}} \geq 4$	
b -tagged jets	$N_{b\text{-jets}} \geq 1$	
Large- R jets	$N_{\text{jets}}^{\text{large}} \geq 1$	
	$E_{\text{T}}^{\text{miss}} \geq 60 \text{ GeV}$	
	$S_{\text{T}} \geq 1200 \text{ GeV}$	
Event kinematics	$N_{\text{jets}}^{\text{large}} \geq 3$ $N_{W_{\text{had}}} \geq 1$ $\Delta R(\text{lep, leading } b\text{-jet}) \geq 1$ $S_{\text{T}} \geq 1500 \text{ GeV}$	veto events in RECOSR

Table 1. Summary of the event selection requirements of the two signal regions.

the transverse momenta of the lepton and all small- R jets. In this context, S_{T} is required to be greater than 1200 GeV.

Assuming exactly one neutrino is present in each event, its four-momentum can be analytically determined using the missing transverse momentum vector $\vec{E}_{\text{T}}^{\text{miss}}$ and assuming the lepton-neutrino system has an invariant mass equal to that of the W boson. Nearly half of the events are found to produce two complex solutions. When complex solutions are obtained, a real solution is determined by minimising a χ^2 parameter based on the difference between the mass of the lepton-neutrino system and the nominal value of the W boson mass. In the case of two real solutions, the solution with the smaller absolute value of the longitudinal momentum is used.

After this selection, backgrounds with large contributions include $t\bar{t}$, $W + \text{jets}$, and single-top events. Other SM processes, including diboson, $Z + \text{jets}$, $t\bar{t}V$ and multi-jet production, make a smaller but non-negligible contribution.

5.2 Classification of event topologies

Two orthogonal signal regions are defined. The reconstructed signal region (RECOSR) aims to reconstruct the $B\bar{B}$ system, whereas the more inclusive signal region (BDTSR) uses a BDT to discriminate between SM and VLQ events. For signal models with $\mathcal{B}(B \rightarrow Wt) = 1$ the relative importance of both signal regions in the final combined fit is roughly equal. In contrast, for SU(2) singlet B scenarios the BDTSR dominates. A summary of the event selection requirements is given in table 1 and the two signal regions are described in detail in section 5.2.1 and section 5.2.2.

5.2.1 RECOSR definition

After the event preselection described in section 5.1, further requirements are applied to reduce the contamination from SM backgrounds in events with at least three reconstructed large- R jets, where at least one is required to be tagged as a W_{had} . Events are required

Sample	Pre-fit		Post-fit	
	RECOSR	BDTSR	RECOSR	BDTSR
$t\bar{t}$	20.2 ± 16.0	$21\,200 \pm 7300$	19.2 ± 5.2	$18\,300 \pm 1500$
$W + \text{jets}$	4.5 ± 2.7	4500 ± 2500	3.6 ± 2.0	3600 ± 1900
Single top	2.4 ± 2.4	2100 ± 1700	0.8 ± 1.0	1000 ± 800
Others	2.7 ± 1.3	n/a	2.7 ± 1.1	n/a
Diboson	n/a	360 ± 200	n/a	340 ± 190
$t\bar{t}V$	n/a	351 ± 57	n/a	350 ± 60
$Z + \text{jets}$	n/a	310 ± 180	n/a	300 ± 170
Multi-jet	n/a	2500 ± 1300	n/a	2000 ± 850
Total background	30.0 ± 16.0	$31\,300 \pm 8200$	26.3 ± 6.3	$25\,900 \pm 400$
Signal ($\mathcal{B}(B \rightarrow Wt) = 1$)	7.4 ± 0.5	51 ± 2	n/a	n/a
Signal (SU(2) singlet)	2.7 ± 0.2	35 ± 1	n/a	n/a
Data	26	25 863	26	25 863

Table 2. Event yields in the two signal regions before and after the background-only fit (see 7.2). The quoted uncertainties include statistical and systematic uncertainties; for the $t\bar{t}$ background no cross-section uncertainty is included since it is a free parameter of the fit. The contributions from dibosons, $Z+\text{jets}$, $t\bar{t}V$ and multi-jet production are included in the ‘Others’ category for the RECOSR, whereas they are counted separately within the BDTSR. Modelling errors on the small $t\bar{t}V$ background are neglected. In the post-fit case, the uncertainties in the individual background components can be larger than the uncertainty in the sum of the backgrounds, which is constrained by data. Both signal models correspond to $m_B = 1300$ GeV.

to have $\Delta R(\text{lep, leading } b\text{-jet}) \geq 1$, as the leading b -jet is found to be well separated from the lepton in VLQ candidates. In addition, S_T is required to be greater than 1500 GeV. These requirements are found to maximise the expected sensitivity to VLQ masses above 1300 GeV for events with at least three reconstructed large- R jets.

The expected number of events in the RECOSR for the background processes and signal hypothesis with mass $m_B = 1300$ GeV are shown in table 2. For a signal model with $\mathcal{B}(B \rightarrow Wt) = 1$, the acceptance times efficiency of the full event selection ranges from 0.2% to 4% for VLQ masses from $m_B = 500$ to 1800 GeV. For the SU(2) singlet B scenario, for which $\mathcal{B}(B \rightarrow Wt)$ is approximately 50% for this mass range, the signal acceptance ranges from 0.1% to 2%. In this signal region, SM processes such as diboson, $Z + \text{jets}$, $t\bar{t}V$, and multi-jet production, make a smaller but non-negligible contribution, and are therefore collectively referred to as ‘Others’.

After the event selection, the four-momenta of the hadronic and semileptonic VLQ candidates are reconstructed using the selected large- R jets and the leptonically decaying W boson candidate. The selected large- R jets are proxies for the hadronically decaying W bosons and top quarks. The leptonically decaying W boson (W_{lep}) candidate is reconstructed from the lepton and reconstructed neutrino. The W_{lep} is paired with a large- R jet to form the semileptonically decaying VLQ candidate. Two additional large- R jets are combined to form the hadronically decaying VLQ candidate. All possible large- R jet

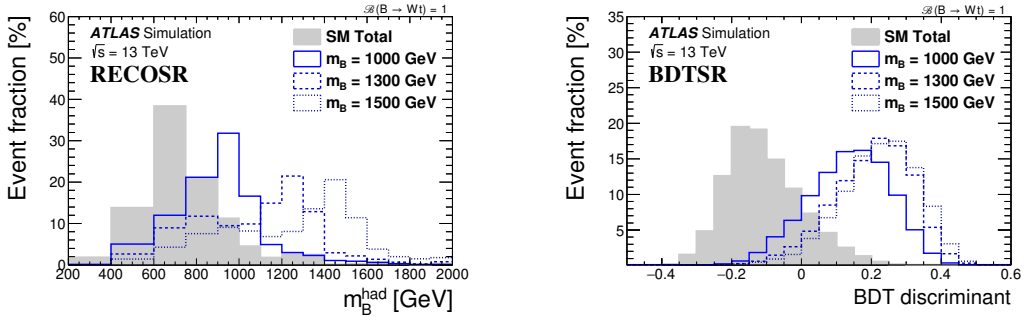


Figure 2. The reconstructed hadronic B quark mass in RECOSR (left) and the BDT discriminant in BDTSR (right) is shown for the total expected background and selected signal mass points for signal models with $\mathcal{B}(B \rightarrow Wt) = 1$. In both figures, the distributions are normalised to unity for comparison of the relative shapes at each mass point.

permutations are tested and the pairing that minimises the absolute value of the mass difference between the semileptonically and hadronically reconstructed VLQ candidates, $|\Delta m|$, is chosen. It should be noted that in cases where the lepton originates from the decay of a top quark, the reconstruction described above neglects the presence of the additional b -jet. This was found to nonetheless provide on average the best separation between signal and background.

The final discriminating variable used in the statistical analysis is m_B^{had} , the reconstructed mass of the hadronically decaying vector-like B quark candidate. This is found to provide good expected signal sensitivity. Figure 2 (left) shows m_B^{had} for benchmark B quark signal models and the total expected background in the RECOSR after the reconstruction algorithm is applied. The reconstructed masses for the signal are shown to peak at the generated B quark masses. The tails arise from misreconstructed B candidates.

5.2.2 BDTSR definition

The BDTSR is defined by all events passing the preselection requirements (section 5.1), but vetoing events contained in the RECOSR. It contains events with less than three large- R jets and thus it is not possible to reconstruct the full $B\bar{B}$ system from the reconstructed objects alone. As a result, a BDT as implemented in the toolkit for multivariate data analysis with ROOT (TMVA) [74] is used to discriminate between potential signal and background events. For training and testing, a set of signal simulation samples assuming $\mathcal{B}(B \rightarrow Wt) = 1$ is used, combining signal masses ranging from 1050 GeV to 1600 GeV. Simulated $t\bar{t}$ events are used as background in the training, as they are the dominant background contribution in this region. Starting from a list of 75 variables describing the kinematics of the event, individual variables are removed through an iterative process and the performance of the BDT is evaluated, until a final set of 20 variables is selected. The procedure for removing variables is based on a combination of poor separation power, or high correlation with a variable with higher separation power, particularly if the correlation is similar between signal and background. Variables with poor agreement between data and simulation are also rejected. The 20 remaining input variables are well modelled by the

simulation. The selected variables describe the global event characteristics as well as the kinematics and angular separation of the reconstructed objects. The five highest-ranked variables are: S_T , the invariant mass of the highest- p_T large- R jet, the sphericity of the event,³ ΔR between the lepton and the sub-leading small- R jet, and ΔR between the leading b -tagged jet and the leading large- R jet.

The expected numbers of events in the BDTSR for the background processes and signal hypothesis with mass $m_B = 1300$ GeV are shown in table 2. For a signal model with $\mathcal{B}(B \rightarrow Wt) = 1$, the acceptance times efficiency of the full event selection ranges from 7% to 24% for VLQ masses from $m_B = 500$ to 1800 GeV. For the SU(2) singlet B scenario the signal acceptance ranges from 4% to 16%.

The final discriminating variable used in the statistical analysis is the BDT discriminant, which is shown in figure 2 (right) for benchmark B quark signal models and the total expected background.

5.3 Multi-jet background estimation

The multi-jet background originates from either the misidentification of a jet or photon as a lepton candidate (fake lepton) or from the presence of a non-prompt lepton (e.g. from a semileptonic b - or c -hadron decay) that passes the isolation requirement. The multi-jet shape, normalisation, and related systematic uncertainties are estimated from data using the matrix method (MM) [76]. The MM exploits the difference in efficiency for prompt leptons to pass loose and tight quality requirements, obtained from W and Z boson decays, and non-prompt or fake lepton candidates, from the misidentification of photons or jets. The efficiencies, measured in dedicated control regions, are parameterised as functions of the lepton candidate p_T and η , $\Delta\phi$ between the lepton and jets, and the b -tagged jet multiplicity.

The event selection significantly reduces the contribution of the multi-jet background in the RECOSR, to the point where statistical uncertainties make the MM prediction unreliable. To obtain a reliable prediction, the requirement on the W -tagged large- R jet is removed. In this region the MM prediction and the small simulation-derived backgrounds (diboson, $Z+jets$ and $t\bar{t}V$) are studied and their distribution shapes of the final discriminant m_B^{had} are found to be compatible. This selection is also used to determine the ratio of the multi-jet production to the small simulation-derived backgrounds. The ratio is then assumed to be the same in the RECOSR and is used to scale those small simulation-derived backgrounds to account for the additional contribution from multi-jet backgrounds. This scaling was found to be stable under small changes to the definition of the looser selection. In the RECOSR region, the contribution from the multi-jet background to the total background is around 1.3%. In the BDTSR, in contrast, the contribution of the multi-jet background is taken directly from the MM prediction

³Sphericity ($\mathcal{S} = \frac{2}{3}(\lambda_2 + \lambda_3)$) is a measure of the total momentum transverse to the sphericity axis defined by the four-momenta used for the event-shape measurement; $\lambda_{2,3}$ are the two smallest eigenvalues of the normalised momentum tensor of the small- R jets, the lepton and the neutrino [75].

6 Systematic uncertainties

The systematic uncertainties are broken down into four broad categories: luminosity and cross-section uncertainties, detector-related experimental uncertainties, uncertainties in data-driven background estimations, and modelling uncertainties in simulated background processes. Each source of uncertainty is treated as a nuisance parameter in the fit of the hadronic B mass and BDT discriminant distributions, and shape effects are taken into account where relevant. Due to the tight selection criteria applied, the systematic uncertainties only mildly degrade the sensitivity of the search.

6.1 Luminosity and normalisation uncertainties

The uncertainty in the combined 2015+2016 integrated luminosity is 2.1%. It is derived, following a methodology similar to that detailed in ref. [77], from a preliminary calibration of the luminosity scale using x - y beam-separation scans performed in August 2015 and May 2016. This systematic uncertainty is applied to all backgrounds and signals that are estimated using simulated Monte Carlo events, which are normalised to the measured integrated luminosity.

Theoretical cross-section uncertainties are applied to the relevant simulated samples. The uncertainties for $W/Z + \text{jets}$ and diboson production are 50% [78, 79]. The uncertainty in the $W + \text{jets}$ normalisation has a pre-fit impact⁴ of 8% on the measured signal strength for a B quark mass of 1.3 TeV ($\mathcal{B}(B \rightarrow Wt) = 1$). This same signal mass and branching ratio is used to quantify the impact of the uncertainties for the remainder of this section. For single top production, the uncertainties are taken as 7% [46, 47]. The normalisation of $t\bar{t}$ is determined from the fit. For the data-driven multi-jet estimation, an uncertainty of 100% is assigned to the normalisation in the RECOSR, corresponding to the maximum range obtained by varying the requirements on S_T and $\Delta R(\text{lep}, \text{leading } b\text{-jet})$ when obtaining the multi-jet contribution from the ‘Others’ background. The corresponding uncertainty in the BDTSR is 50% and evaluated by comparing the data with simulation in a region enriched in multi-jet events.

6.2 Detector-related uncertainties

The dominant sources of detector-related uncertainties in the signal and background yields relate to the small- R and large- R jet energy scales and resolutions. The small- R and large- R jet energy scales and their uncertainties are derived by combining information from test-beam data, LHC collision data and simulation [80]. In addition to energy scale and resolution uncertainties, there are also uncertainties in the large- R jet mass and substructure scales and resolutions. These are evaluated in a similar way to the jet energy scale and resolution uncertainties and are propagated to the W -tagging efficiencies. The uncertainty in the large- R jet kinematics due to differences between data and simulation seen in

⁴The pre-fit effect on the signal strength parameter μ is calculated by fixing the corresponding nuisance parameter at $\theta \pm \sigma_\theta$, where θ is the initial value of the nuisance parameter and σ_θ is its pre-fit uncertainty, and performing the fit again. The difference between the default and the modified value of μ , $\Delta\mu$, represents the effect on μ of this particular uncertainty (see section 7.1 for further details).

the large- R jet calibration analysis has the largest pre-fit impact on the measured signal strength, at $\sim 12\%$.

Other detector-related uncertainties come from lepton trigger efficiencies, identification efficiencies, energy scales and resolutions, the E_T^{miss} reconstruction, the b -tagging efficiency, and the JVT requirement. These have negligible pre-fit impact on the measured signal strength ($< 1\%$).

6.3 Generator modelling uncertainties

Modelling uncertainties are estimated for the dominant $t\bar{t}$ and single-top backgrounds. The modelling uncertainties are estimated by comparing simulated samples generated with different configurations, described in section 3. The effects of extra initial- and final-state gluon radiation are estimated by comparing simulated samples generated with enhanced or reduced initial-state radiation, changes to the h_{damp} parameter, and different values of the radiation parameters. This uncertainty has a 30% and 20% normalisation impact on $t\bar{t}$ in the RECOSR and BDTSR, respectively, resulting in a pre-fit impact of $\sim 3\%$ on the measured signal strength.⁵ The uncertainty in the fragmentation, hadronisation and underlying-event modelling is estimated by comparing two different parton shower models, PYTHIA and HERWIG 7, while keeping the same hard-scatter matrix-element generator. This causes a 55% and 5% shift in the normalisation of $t\bar{t}$ in the RECOSR and BDTSR, respectively, resulting in a pre-fit impact of 9% on the measured signal strength. The uncertainty in the hard-scatter generation is estimated by comparing events generated with two different Monte Carlo generators, MADGRAPH5_aMC@NLO and POWHEG-Box, while keeping the same parton shower model. This uncertainty has a 27% normalisation impact on $t\bar{t}$ in both signal regions, resulting in a pre-fit impact of $\sim 4\%$ on the measured signal strength.

For single top production, the dominant contribution in this analysis is from Wt production and the largest uncertainty comes from the method used to remove the overlap between NLO Wt production and LO $t\bar{t}$ production. The default method of diagram removal is compared with the alternative method of diagram subtraction [45]. The full difference between the two methods is assigned as an uncertainty. This uncertainty has a 90% and 80% normalisation impact on single top in the RECOSR and BDTSR, respectively, resulting in a pre-fit impact of $\sim 16\%$ on the measured signal strength.

7 Results

7.1 Statistical interpretation

The binned distributions of the reconstructed mass of the hadronically decaying B quark candidate, m_B^{had} , in the RECOSR, and of the BDT discriminant in the BDTSR, are used to test for the presence of a signal. Hypothesis testing is performed using a modified frequentist method as implemented in RooStats [81, 82] and is based on a profile likelihood that

⁵The impact on the $t\bar{t}$ normalisation is provided for illustration purposes only, as the overall $t\bar{t}$ normalisation is a free parameter of the fit.

takes into account the systematic uncertainties as nuisance parameters that are fitted to the data. A simultaneous fit is performed in the two signal regions. The number and edges of the bins are optimised to maximise the expected vector-like B quark sensitivity while ensuring the overall Monte Carlo statistical uncertainty in each bin remains below 30%.

The statistical analysis is based on a binned likelihood function $\mathcal{L}(\mu, \theta)$ constructed as a product of Poisson probability terms over all bins considered in the search. This function depends on the signal strength parameter μ , a multiplicative factor applied to the theoretical signal production cross-section, and θ , a set of nuisance parameters that encode the effect of systematic uncertainties in the signal and background expectations and are implemented in the likelihood function as Gaussian constraints. Uncertainties in each bin of the fitted distributions due to the finite size of the simulated event samples are also taken into account via additional dedicated fit parameters and are propagated to μ . There are enough events in the low mass and low BDT score regions, where the signal contribution is small, to obtain a data-driven estimate of the $t\bar{t}$ normalisation and hence the normalisation of the dominant $t\bar{t}$ background is included as an unconstrained nuisance parameter. Nuisance parameters representing systematic uncertainties are only included in the likelihood if either of the following conditions are met: the overall impact on the sample normalisation is larger than 1%, or the variation induces changes of more than 1% between adjacent bins. This reduction of the number of nuisance parameter is done separately for the two signal regions and for each template (signal or background). When the bin-by-bin statistical variation of a given uncertainty is significant, a smoothing algorithm is applied.

The expected number of events in a given bin depends on μ and θ . The nuisance parameters θ adjust the expectations for signal and background according to the corresponding systematic uncertainties, and their values correspond to the values that best fit the data.

The test statistic q_μ is defined as the profile likelihood ratio, $q_\mu = -2\ln(\mathcal{L}(\mu, \hat{\theta}_\mu)/\mathcal{L}(\hat{\mu}, \hat{\theta}))$, where $\hat{\mu}$ and $\hat{\theta}$ are the values of the parameters that maximise the likelihood function (with the constraint $0 \leq \hat{\mu} \leq \mu$), and $\hat{\theta}_\mu$ are the values of the nuisance parameters that maximise the likelihood function for a given value of μ . The compatibility of the observed data with the background-only hypothesis is tested by setting $\mu = 0$ in the profile likelihood ratio: $q_0 = -2\ln(\mathcal{L}(0, \hat{\theta}_0)/\mathcal{L}(\hat{\mu}, \hat{\theta}))$. Upper limits on the signal production cross-section for each of the signal scenarios considered are derived by using q_μ in the CL_s method [83, 84]. For a given signal scenario, values of the production cross-section (parameterised by μ) yielding $\text{CL}_s < 0.05$, where CL_s is computed using the asymptotic approximation [85], are excluded at $\geq 95\%$ CL.

7.2 Likelihood fit results

The expected and observed event yields in both signal regions after fitting the background-only hypothesis to data, including all uncertainties, are listed in table 2. The total uncertainty shown in the table is the uncertainty obtained from the full fit, and is therefore not identical to the sum in quadrature of all components, due to the correlations between the fit parameters. The probability that the data is compatible with the background-only

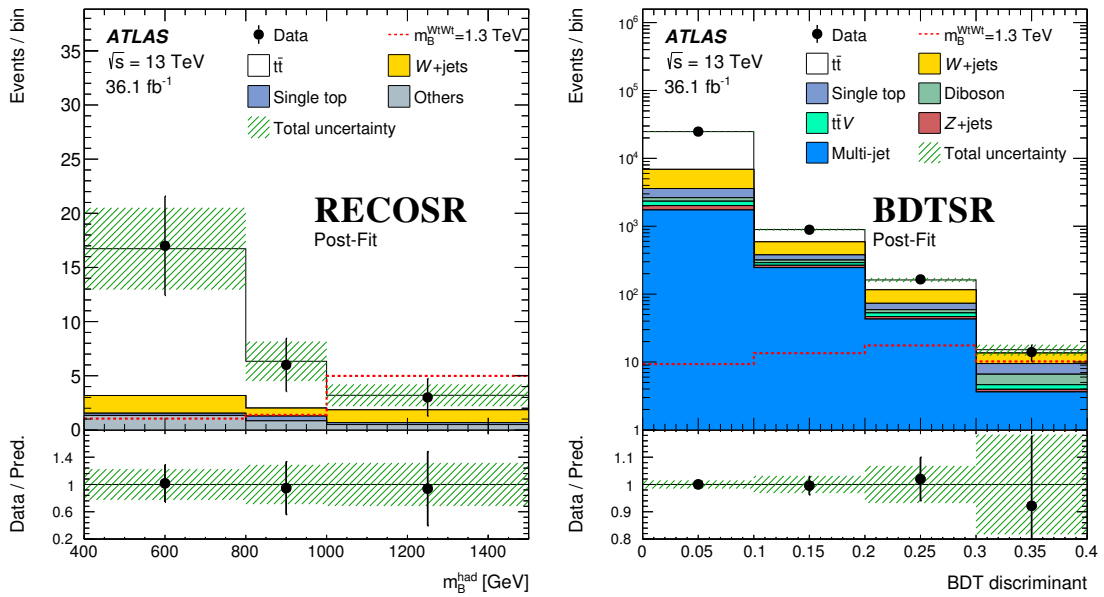


Figure 3. Fit results (background-only) for the hadronic B quark candidate mass distributions m_B^{had} (left) and the BDT discriminant in BDTSR (right). The lower panel shows the ratio of data to the fitted background yields. The band represents the total uncertainty after the maximum-likelihood fit. Events in the overflow and underflow bins are included in the last and first bin of the histograms, respectively. The expected $B\bar{B}$ signal corresponding to $m_B = 1300$ GeV for a branching ratio of 100% into $WtWt$ is also shown overlaid.

hypothesis is estimated by integrating the distribution of the test statistic, approximated using the asymptotic formulae [85], above the observed value of q_0 . This value is computed for each signal scenario considered, defined by the assumed mass of the heavy quark and the three decay branching ratios. The lowest p -value is found to be $\sim 50\%$, for a B mass of 800 GeV. Thus no significant excess above the background expectation is found.

Individual uncertainties are generally not significantly constrained by data, except for the uncertainty associated with the single top modelling, which is constrained to be within 50% of its initial size.

A comparison of the post-fit agreement between data and prediction for both regions is shown in figure 3. The RECOUSR shows a slight deficit of data for the m_B^{had} distribution above 800 GeV. Hence, the observed upper limits on the $B\bar{B}$ production cross-section are slightly stronger than the expected sensitivity. The post-fit $t\bar{t}$ normalisation in these regions is found to be 0.92 ± 0.30 times the Monte Carlo prediction, normalised to the NNLO+NNLL cross-section.

7.3 Limits on VLQ pair production

Upper limits at the 95% CL on the $B\bar{B}$ production cross-section are set for two benchmark scenarios as a function of B quark mass m_B and compared with the theoretical prediction from TOP++ v2.0 (figure 4). The resulting lower limit on m_B is determined using the central value of the theoretical cross-section prediction. These results are only valid for new

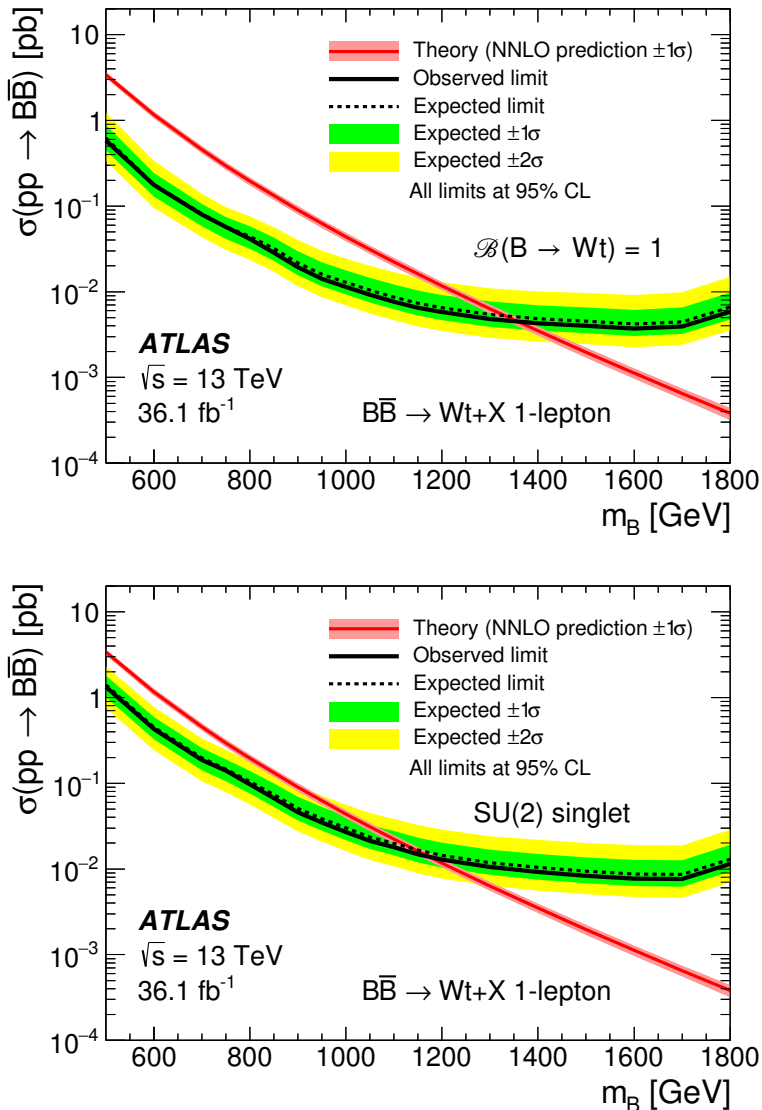


Figure 4. Observed (solid line) and expected (dashed line) 95% CL upper limits on the $B\bar{B}$ cross-section as a function of B quark mass assuming $\mathcal{B}(B \rightarrow Wt) = 1$ (top) and in the SU(2) singlet B scenario (bottom). The surrounding shaded bands correspond to ± 1 and ± 2 standard deviations around the expected limit. The red line and band show the theoretical prediction and its ± 1 standard deviation uncertainty.

particles of narrow width. Assuming $\mathcal{B}(B \rightarrow Wt) = 1$, the observed (expected) lower limit is $m_B = 1350$ GeV (1330 GeV). For branching ratios corresponding to the SU(2) singlet B scenario, the observed (expected) 95% CL lower limit is $m_B = 1170$ GeV (1140 GeV). These represent a significant improvement over the reinterpreted search [17], for which the observed 95% CL limit was 1250 GeV when assuming $\mathcal{B}(B \rightarrow Wt) = 1$.

To check that the results do not depend on the weak-isospin of the B quark in the simulated signal events, a sample of $B\bar{B}$ events with a mass of 1200 GeV was generated for an SU(2) (T_B) doublet B quark and compared with the nominal sample of the same mass

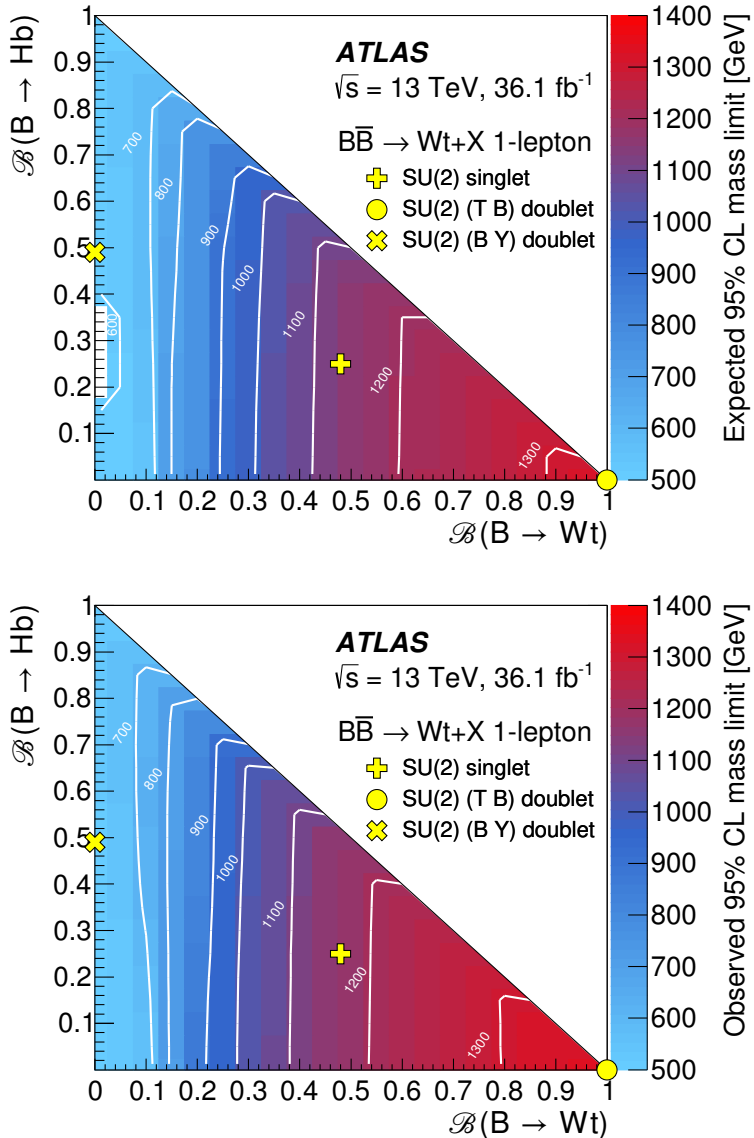


Figure 5. Expected (top) and observed (bottom) 95% CL lower limits on the mass of the B quark as a function of the decay branching ratios $\mathcal{B}(B \rightarrow Wt)$ and $\mathcal{B}(B \rightarrow Hb)$. The white contour lines represent constant mass limits. The markers indicate the branching ratios for the SU(2) singlet and both SU(2) doublet scenarios with masses above ~ 800 GeV, where they are approximately independent of the VLQ B mass. The small white region in the upper plot is due to the limit falling below 500 GeV, the lowest simulated signal mass.

generated for an SU(2) singlet B quark. Both the expected number of events and expected excluded cross-section are found to be consistent between those two samples. Thus the limits obtained are also applicable to VLQ models with non-zero weak-isospin. As there is no explicit use of charge identification, the $\mathcal{B}(B \rightarrow Wt) = 1$ limits are found to be applicable to pair-produced vector-like X quarks of charge +5/3 which decay exclusively into Wt .

Exclusion limits on B quark pair production are also obtained for different values of m_B and as a function of branching ratios to each of the three decays. In order to probe the complete branching-ratio plane, the signal samples are weighted by the ratios of the respective branching ratios to the original branching ratios in PROTOS. Then, the complete analysis is repeated for each point in the branching-ratio plane. Figure 5 shows the corresponding expected and observed B quark mass limits in the plane $\mathcal{B}(B \rightarrow Hb)$ versus $\mathcal{B}(B \rightarrow Wt)$, obtained by linear interpolation of the calculated CL_s versus m_B .

8 Conclusions

A search for the pair production of a heavy vector-like B quark, based on pp collisions at $\sqrt{s} = 13$ TeV recorded in 2015 (3.2 fb^{-1}) and 2016 (32.9 fb^{-1}) with the ATLAS detector at the CERN Large Hadron Collider, is presented. Data are analysed in the lepton-plus-jets final state and no significant deviation from the Standard Model expectation is observed. Assuming a branching ratio $\mathcal{B}(B \rightarrow Wt) = 1$, the observed (expected) 95% CL lower limit on the vector-like quark mass is 1350 GeV (1330 GeV). For the scenario of an SU(2) singlet B quark, the observed (expected) mass limit is 1170 GeV (1140 GeV). Assuming the B quark can only decay into Wt , Zb and Hb , 95% CL lower limits are derived for various masses in the two-dimensional plane of $\mathcal{B}(B \rightarrow Wt)$ versus $\mathcal{B}(B \rightarrow Hb)$. The limit for $\mathcal{B}(B \rightarrow Wt) = 1$ is found to be equally applicable to VLQ X quarks that decay into Wt .

Acknowledgments

We thank CERN for the very successful operation of the LHC, as well as the support staff from our institutions without whom ATLAS could not be operated efficiently.

We acknowledge the support of ANPCyT, Argentina; YerPhI, Armenia; ARC, Australia; BMWFW and FWF, Austria; ANAS, Azerbaijan; SSTC, Belarus; CNPq and FAPESP, Brazil; NSERC, NRC and CFI, Canada; CERN; CONICYT, Chile; CAS, MOST and NSFC, China; COLCIENCIAS, Colombia; MSMT CR, MPO CR and VSC CR, Czech Republic; DNRF and DNSRC, Denmark; IN2P3-CNRS, CEA-DRF/IRFU, France; SRNSFG, Georgia; BMBF, HGF, and MPG, Germany; GSRT, Greece; RGC, Hong Kong SAR, China; ISF, I-CORE and Benoziyo Center, Israel; INFN, Italy; MEXT and JSPS, Japan; CNRST, Morocco; NWO, Netherlands; RCN, Norway; MNiSW and NCN, Poland; FCT, Portugal; MNE/IFA, Romania; MES of Russia and NRC KI, Russian Federation; JINR; MESTD, Serbia; MSSR, Slovakia; ARRS and MIZŠ, Slovenia; DST/NRF, South Africa; MINECO, Spain; SRC and Wallenberg Foundation, Sweden; SERI, SNSF and Cantons of Bern and Geneva, Switzerland; MOST, Taiwan; TAEK, Turkey; STFC, United Kingdom; DOE and NSF, United States of America. In addition, individual groups and members have received support from BCKDF, the Canada Council, CANARIE, CRC, Compute Canada, FQRNT, and the Ontario Innovation Trust, Canada; EPLANET, ERC, ERDF, FP7, Horizon 2020 and Marie Skłodowska-Curie Actions, European Union; Investissements d’Avenir Labex and Idex, ANR, Région Auvergne and Fondation Partager le Savoir, France; DFG and AvH Foundation, Germany; Herakleitos, Thales and Aristea

programmes co-financed by EU-ESF and the Greek NSRF; BSF, GIF and Minerva, Israel; BRF, Norway; CERCA Programme Generalitat de Catalunya, Generalitat Valenciana, Spain; the Royal Society and Leverhulme Trust, United Kingdom.

The crucial computing support from all WLCG partners is acknowledged gratefully, in particular from CERN, the ATLAS Tier-1 facilities at TRIUMF (Canada), NDGF (Denmark, Norway, Sweden), CC-IN2P3 (France), KIT/GridKA (Germany), INFN-CNAF (Italy), NL-T1 (Netherlands), PIC (Spain), ASGC (Taiwan), RAL (U.K.) and BNL (U.S.A.), the Tier-2 facilities worldwide and large non-WLCG resource providers. Major contributors of computing resources are listed in ref. [86].

Open Access. This article is distributed under the terms of the Creative Commons Attribution License ([CC-BY 4.0](#)), which permits any use, distribution and reproduction in any medium, provided the original author(s) and source are credited.

References

- [1] ATLAS collaboration, *Observation of a new particle in the search for the standard model Higgs boson with the ATLAS detector at the LHC*, *Phys. Lett. B* **716** (2012) 1 [[arXiv:1207.7214](#)] [[INSPIRE](#)].
- [2] CMS collaboration, *Observation of a new boson at a mass of 125 GeV with the CMS experiment at the LHC*, *Phys. Lett. B* **716** (2012) 30 [[arXiv:1207.7235](#)] [[INSPIRE](#)].
- [3] G. 't Hooft, in *Recent developments in gauge theories*, G. 't Hooft et al. eds., Plenum, New York U.S.A. (1980).
- [4] N. Arkani-Hamed, A.G. Cohen, E. Katz and A.E. Nelson, *The littlest Higgs*, *JHEP* **07** (2002) 034 [[hep-ph/0206021](#)] [[INSPIRE](#)].
- [5] M. Schmaltz and D. Tucker-Smith, *Little Higgs review*, *Ann. Rev. Nucl. Part. Sci.* **55** (2005) 229 [[hep-ph/0502182](#)] [[INSPIRE](#)].
- [6] D.B. Kaplan, H. Georgi and S. Dimopoulos, *Composite Higgs scalars*, *Phys. Lett.* **136B** (1984) 187 [[INSPIRE](#)].
- [7] K. Agashe, R. Contino and A. Pomarol, *The minimal composite Higgs model*, *Nucl. Phys. B* **719** (2005) 165 [[hep-ph/0412089](#)] [[INSPIRE](#)].
- [8] C.T. Hill and E.H. Simmons, *Strong dynamics and electroweak symmetry breaking*, *Phys. Rept.* **381** (2003) 235 [*Erratum ibid. 390 (2004) 553*] [[hep-ph/0203079](#)] [[INSPIRE](#)].
- [9] F. del Aguila and M.J. Bowick, *The possibility of new fermions with $\Delta I = 0$ mass*, *Nucl. Phys. B* **224** (1983) 107 [[INSPIRE](#)].
- [10] J.A. Aguilar-Saavedra, *Identifying top partners at LHC*, *JHEP* **11** (2009) 030 [[arXiv:0907.3155](#)] [[INSPIRE](#)].
- [11] J.A. Aguilar-Saavedra, *Mixing with vector-like quarks: constraints and expectations*, *EPJ Web Conf.* **60** (2013) 16012 [[arXiv:1306.4432](#)] [[INSPIRE](#)].
- [12] J.A. Aguilar-Saavedra et al., *Handbook of vectorlike quarks: mixing and single production*, *Phys. Rev. D* **88** (2013) 094010 [[arXiv:1306.0572](#)] [[INSPIRE](#)].
- [13] A. Atre, M. Carena, T. Han and J. Santiago, *Heavy quarks above the top at the Tevatron*, *Phys. Rev. D* **79** (2009) 054018 [[arXiv:0806.3966](#)] [[INSPIRE](#)].

- [14] A. Atre et al., *Model-independent searches for new quarks at the LHC*, *JHEP* **08** (2011) 080 [[arXiv:1102.1987](#)] [[INSPIRE](#)].
- [15] CMS collaboration, *Search for pair-produced vectorlike B quarks in proton-proton collisions at $\sqrt{s} = 8$ TeV*, *Phys. Rev. D* **93** (2016) 112009 [[arXiv:1507.07129](#)] [[INSPIRE](#)].
- [16] CMS collaboration, *Search for top quark partners with charge 5/3 in proton-proton collisions at $\sqrt{s} = 13$ TeV*, *JHEP* **08** (2017) 073 [[arXiv:1705.10967](#)] [[INSPIRE](#)].
- [17] ATLAS collaboration, *Search for pair production of heavy vector-like quarks decaying to high- p_T W bosons and b quarks in the lepton-plus-jets final state in pp collisions at $\sqrt{s} = 13$ TeV with the ATLAS detector*, *JHEP* **10** (2017) 141 [[arXiv:1707.03347](#)] [[INSPIRE](#)].
- [18] ATLAS collaboration, *Identification of boosted, hadronically-decaying W and Z bosons in $\sqrt{s} = 13$ TeV Monte Carlo Simulations for ATLAS*, ATL-PHYS-PUB-2015-033 (2015).
- [19] ATLAS collaboration, *Boosted hadronic top identification at ATLAS for early 13 TeV data*, ATL-PHYS-PUB-2015-053 (2015).
- [20] ATLAS collaboration, *The ATLAS experiment at the CERN Large Hadron Collider*, *2008 JINST* **3** S08003 [[INSPIRE](#)].
- [21] ATLAS collaboration, *ATLAS insertable B-layer technical design report*, ATL-TDR-19 (2010), and ATL-TDR-19-ADD-1 (2012).
- [22] ATLAS collaboration, *Early inner detector tracking performance in the 2015 data at $\sqrt{s} = 13$ TeV*, ATL-PHYS-PUB-2015-051 (2015).
- [23] ATLAS collaboration, *Performance of the ATLAS Trigger System in 2015*, *Eur. Phys. J. C* **77** (2017) 317 [[arXiv:1611.09661](#)] [[INSPIRE](#)].
- [24] J. Aguilar-Saavedra, *Protos: PROgram for TOp Simulations*, <https://jaguilar.web.cern.ch/jaguilar/protos>.
- [25] R.D. Ball et al., *Parton distributions with LHC data*, *Nucl. Phys. B* **867** (2013) 244 [[arXiv:1207.1303](#)] [[INSPIRE](#)].
- [26] ATLAS collaboration, *ATLAS Run 1 PYTHIA8 tunes*, ATL-PHYS-PUB-2014-021 (2014).
- [27] T. Sjöstrand, S. Mrenna and P.Z. Skands, *A brief introduction to PYTHIA 8.1*, *Comput. Phys. Commun.* **178** (2008) 852 [[arXiv:0710.3820](#)] [[INSPIRE](#)].
- [28] M. Czakon and A. Mitov, *Top++: a program for the calculation of the top-pair cross-section at hadron colliders*, *Comput. Phys. Commun.* **185** (2014) 2930 [[arXiv:1112.5675](#)] [[INSPIRE](#)].
- [29] M. Cacciari, M. Czakon, M. Mangano, A. Mitov and P. Nason, *Top-pair production at hadron colliders with next-to-next-to-leading logarithmic soft-gluon resummation*, *Phys. Lett. B* **710** (2012) 612 [[arXiv:1111.5869](#)] [[INSPIRE](#)].
- [30] M. Beneke, P. Falgari, S. Klein and C. Schwinn, *Hadronic top-quark pair production with NNLL threshold resummation*, *Nucl. Phys. B* **855** (2012) 695 [[arXiv:1109.1536](#)] [[INSPIRE](#)].
- [31] P. Bärnreuther, M. Czakon and A. Mitov, *Percent level precision physics at the Tevatron: first genuine NNLO QCD corrections to $q\bar{q} \rightarrow t\bar{t} + X$* , *Phys. Rev. Lett.* **109** (2012) 132001 [[arXiv:1204.5201](#)] [[INSPIRE](#)].
- [32] M. Czakon and A. Mitov, *NNLO corrections to top-pair production at hadron colliders: the all-fermionic scattering channels*, *JHEP* **12** (2012) 054 [[arXiv:1207.0236](#)] [[INSPIRE](#)].

- [33] M. Czakon and A. Mitov, *NNLO corrections to top pair production at hadron colliders: the quark-gluon reaction*, *JHEP* **01** (2013) 080 [[arXiv:1210.6832](#)] [[INSPIRE](#)].
- [34] M. Czakon, P. Fiedler and A. Mitov, *Total top-quark pair-production cross section at hadron colliders through $O(\alpha_s^4)$* , *Phys. Rev. Lett.* **110** (2013) 252004 [[arXiv:1303.6254](#)] [[INSPIRE](#)].
- [35] A.D. Martin et al., *Heavy-quark mass dependence in global PDF analyses and 3- and 4-flavour parton distributions*, *Eur. Phys. J. C* **70** (2010) 51 [[arXiv:1007.2241](#)].
- [36] M. Botje et al., *The PDF4LHC working group interim recommendations*, [arXiv:1101.0538](#) [[INSPIRE](#)].
- [37] H.-L. Lai et al., *New parton distributions for collider physics*, *Phys. Rev. D* **82** (2010) 074024 [[arXiv:1007.2241](#)] [[INSPIRE](#)].
- [38] J. Gao et al., *CT10 next-to-next-to-leading order global analysis of QCD*, *Phys. Rev. D* **89** (2014) 033009 [[arXiv:1302.6246](#)] [[INSPIRE](#)].
- [39] S. Alioli et al., *A general framework for implementing NLO calculations in shower Monte Carlo programs: the POWHEG BOX*, *JHEP* **06** (2010) 043 [[arXiv:1002.2581](#)] [[INSPIRE](#)].
- [40] T. Sjöstrand et al., *An Introduction to PYTHIA 8.2*, *Comput. Phys. Commun.* **191** (2015) 159 [[arXiv:1410.3012](#)] [[INSPIRE](#)].
- [41] G. Corcella et al., *HERWIG 6: An Event generator for hadron emission reactions with interfering gluons (including supersymmetric processes)*, *JHEP* **01** (2001) 010 [[hep-ph/0011363](#)] [[INSPIRE](#)].
- [42] J. Alwall et al., *The automated computation of tree-level and next-to-leading order differential cross sections and their matching to parton shower simulations*, *JHEP* **07** (2014) 079 [[arXiv:1405.0301](#)] [[INSPIRE](#)].
- [43] T. Sjöstrand et al., *High-energy physics event generation with PYTHIA 6.1*, *Comput. Phys. Commun.* **135** (2001) 238 [[hep-ph/0010017](#)] [[INSPIRE](#)].
- [44] P.Z. Skands, *Tuning Monte Carlo generators: the Perugia tunes*, *Phys. Rev. D* **82** (2010) 074018 [[arXiv:1005.3457](#)] [[INSPIRE](#)].
- [45] S. Frixione et al., *Single-top hadroproduction in association with a W boson*, *JHEP* **07** (2008) 029 [[arXiv:0805.3067](#)] [[INSPIRE](#)].
- [46] M. Aliev et al., *HATHOR: HAdronic Top and Heavy quarks crOss section calculatoR*, *Comput. Phys. Commun.* **182** (2011) 1034 [[arXiv:1007.1327](#)] [[INSPIRE](#)].
- [47] P. Kant et al., *Hathor for single top-quark production: Updated predictions and uncertainty estimates for single top-quark production in hadronic collisions*, *Comput. Phys. Commun.* **191** (2015) 74 [[arXiv:1406.4403](#)] [[INSPIRE](#)].
- [48] N. Kidonakis, *Next-to-next-to-leading-order collinear and soft gluon corrections for t-channel single top quark production*, *Phys. Rev. D* **83** (2011) 091503 [[arXiv:1103.2792](#)] [[INSPIRE](#)].
- [49] T. Gleisberg et al., *Event generation with SHERPA 1.1*, *JHEP* **02** (2009) 007 [[arXiv:0811.4622](#)] [[INSPIRE](#)].
- [50] C. Anastasiou et al., *High precision QCD at hadron colliders: electroweak gauge boson rapidity distributions at NNLO*, *Phys. Rev. D* **69** (2004) 094008 [[hep-ph/0312266](#)] [[INSPIRE](#)].
- [51] K. Melnikov and F. Petriello, *Electroweak gauge boson production at hadron colliders through $O(\alpha_s^2)$* , *Phys. Rev. D* **74** (2006) 114017 [[hep-ph/0609070](#)] [[INSPIRE](#)].

- [52] R. Gavin et al., *FEWZ 2.0: a code for hadronic Z production at next-to-next-to-leading order*, *Comput. Phys. Commun.* **182** (2011) 2388 [[arXiv:1011.3540](#)] [[INSPIRE](#)].
- [53] D.J. Lange, *The EvtGen particle decay simulation package*, *Nucl. Instrum. Meth. A* **462** (2001) 152 [[INSPIRE](#)].
- [54] ATLAS collaboration, *The ATLAS simulation infrastructure*, *Eur. Phys. J. C* **70** (2010) 823 [[arXiv:1005.4568](#)] [[INSPIRE](#)].
- [55] GEANT4 collaboration, S. Agostinelli et al., *GEANT4 — a simulation toolkit*, *Nucl. Instrum. Meth. A* **506** (2003) 250 [[INSPIRE](#)].
- [56] ATLAS collaboration, *The simulation principle and performance of the ATLAS fast calorimeter simulation FastCaloSim*, [ATL-PHYS-PUB-2010-013](#) (2010).
- [57] ATLAS collaboration, *Summary of ATLAS PYTHIA 8 tunes*, [ATL-PHYS-PUB-2012-003](#) (2012).
- [58] ATLAS collaboration, *Topological cell clustering in the ATLAS calorimeters and its performance in LHC Run 1*, *Eur. Phys. J. C* **77** (2017) 490 [[arXiv:1603.02934](#)] [[INSPIRE](#)].
- [59] M. Cacciari, G.P. Salam and G. Soyez, *The anti- k_t jet clustering algorithm*, *JHEP* **04** (2008) 063 [[arXiv:0802.1189](#)] [[INSPIRE](#)].
- [60] M. Cacciari and G.P. Salam, *Dispelling the N^3 myth for the k_t jet-finder*, *Phys. Lett. B* **641** (2006) 57 [[hep-ph/0512210](#)] [[INSPIRE](#)].
- [61] M. Cacciari, G.P. Salam and G. Soyez, *FastJet user manual*, *Eur. Phys. J. C* **72** (2012) 1896 [[arXiv:1111.6097](#)] [[INSPIRE](#)].
- [62] ATLAS collaboration, *Jet energy scale measurements and their systematic uncertainties in proton-proton collisions at $\sqrt{s} = 13$ TeV with the ATLAS detector*, *Phys. Rev. D* **96** (2017) 072002 [[arXiv:1703.09665](#)] [[INSPIRE](#)].
- [63] ATLAS collaboration, *Performance of pile-up mitigation techniques for jets in pp collisions at $\sqrt{s} = 8$ TeV using the ATLAS detector*, *Eur. Phys. J. C* **76** (2016) 581 [[arXiv:1510.03823](#)] [[INSPIRE](#)].
- [64] ATLAS collaboration, *Performance of b-jet identification in the ATLAS experiment*, **2016 JINST** **11** P04008 [[arXiv:1512.01094](#)] [[INSPIRE](#)].
- [65] ATLAS collaboration, *Optimisation of the ATLAS b-tagging performance for the 2016 LHC Run*, [ATL-PHYS-PUB-2016-012](#) (2016).
- [66] ATLAS collaboration, *Measurement of b-tagging efficiency of c-jets in $t\bar{t}$ events using a likelihood approach with the ATLAS detector*, [ATLAS-CONF-2018-001](#) (2018).
- [67] D. Krohn, J. Thaler and L.-T. Wang, *Jet trimming*, *JHEP* **02** (2010) 084 [[arXiv:0912.1342](#)] [[INSPIRE](#)].
- [68] A.J. Larkoski, I. Moult and D. Neill, *Power counting to better jet observables*, *JHEP* **12** (2014) 009 [[arXiv:1409.6298](#)] [[INSPIRE](#)].
- [69] A.J. Larkoski, I. Moult and D. Neill, *Analytic boosted boson discrimination*, *JHEP* **05** (2016) 117 [[arXiv:1507.03018](#)] [[INSPIRE](#)].
- [70] ATLAS collaboration, *Jet mass reconstruction with the ATLAS Detector in early Run 2 data*, [ATLAS-CONF-2016-035](#) (2016).

- [71] ATLAS collaboration, *Electron efficiency measurements with the ATLAS detector using the 2015 LHC proton-proton collision data*, [ATLAS-CONF-2016-024](#) (2016).
- [72] ATLAS collaboration, *Muon reconstruction performance of the ATLAS detector in proton-proton collision data at $\sqrt{s} = 13$ TeV*, [Eur. Phys. J. C](#) **76** (2016) 292 [[arXiv:1603.05598](#)] [[INSPIRE](#)].
- [73] ATLAS collaboration, *Performance of missing transverse momentum reconstruction for the ATLAS detector in the first proton-proton collisions at $\sqrt{s} = 13$ TeV*, [ATL-PHYS-PUB-2015-027](#) (2015).
- [74] A. Hocker et al., *TMVA — Toolkit for Multivariate Data Analysis*, [physics/0703039](#) [[INSPIRE](#)].
- [75] J.D. Bjorken and S.J. Brodsky, *Statistical model for electron-positron annihilation into hadrons*, [Phys. Rev. D](#) **1** (1970) 1416 [[INSPIRE](#)].
- [76] ATLAS collaboration, *Measurement of the top quark-pair production cross section with ATLAS in pp collisions at $\sqrt{s} = 7$ TeV*, [Eur. Phys. J. C](#) **71** (2011) 1577 [[arXiv:1012.1792](#)] [[INSPIRE](#)].
- [77] ATLAS collaboration, *Luminosity determination in pp collisions at $\sqrt{s} = 8$ TeV using the ATLAS detector at the LHC*, [Eur. Phys. J. C](#) **76** (2016) 653 [[arXiv:1608.03953](#)] [[INSPIRE](#)].
- [78] ATLAS collaboration, *ATLAS simulation of boson plus jets processes in Run 2*, [ATL-PHYS-PUB-2017-006](#) (2017).
- [79] ATLAS collaboration, *Multi-Boson Simulation for 13 TeV ATLAS Analyses*, [ATL-PHYS-PUB-2016-002](#) (2016).
- [80] ATLAS collaboration, *Jet calibration and systematic uncertainties for jets reconstructed in the ATLAS detector at $\sqrt{s} = 13$ TeV*, [ATL-PHYS-PUB-2015-015](#) (2015).
- [81] W. Verkerke and D.P. Kirkby, *The RooFit toolkit for data modeling*, [eConf C](#) **0303241** (2003) MOLT007 [[physics/0306116](#)] [[INSPIRE](#)].
- [82] W. Verkerke and D. Kirkby, *RooFit users manual v2.91*, <https://rootfit.sourceforge.net>.
- [83] A.L. Read, *Presentation of search results: the CL_s technique*, [J. Phys. G](#) **28** (2002) 2693 [[INSPIRE](#)].
- [84] T. Junk, *Confidence level computation for combining searches with small statistics*, [Nucl. Instrum. Meth. A](#) **434** (1999) 435 [[hep-ex/9902006](#)] [[INSPIRE](#)].
- [85] G. Cowan et al., *Asymptotic formulae for likelihood-based tests of new physics*, [Eur. Phys. J. C](#) **71** (2011) 1554 [Erratum *ibid. C* **73** (2013) 2501] [[arXiv:1007.1727](#)] [[INSPIRE](#)].
- [86] ATLAS collaboration, *ATLAS computing acknowledgements*, [ATL-GEN-PUB-2016-002](#) (2016).

The ATLAS collaboration

M. Aaboud^{34d}, G. Aad⁹⁹, B. Abbott¹²⁴, O. Abdinov^{13,*}, B. Abelsoos¹²⁸, D.K. Abhayasinghe⁹¹, S.H. Abidi¹⁶⁴, O.S. AbouZeid¹⁴³, N.L. Abraham¹⁵³, H. Abramowicz¹⁵⁸, H. Abreu¹⁵⁷, Y. Abulaiti⁶, B.S. Acharya^{64a,64b,o}, S. Adachi¹⁶⁰, L. Adamczyk^{81a}, J. Adelman¹¹⁹, M. Adlersberger¹¹², A. Adiguzel^{12c,ah}, T. Adye¹⁴¹, A.A. Affolder¹⁴³, Y. Afik¹⁵⁷, C. Agheorghiesei^{27c}, J.A. Aguilar-Saavedra^{136f,136a}, F. Ahmadov^{77,af}, G. Aielli^{71a,71b}, S. Akatsu⁸³, T.P.A. Åkesson⁹⁴, E. Akilli⁵², A.V. Akimov¹⁰⁸, G.L. Alberghi^{23b,23a}, J. Albert¹⁷³, P. Albicocco⁴⁹, M.J. Alconada Verzini⁸⁶, S. Alderweireldt¹¹⁷, M. Alekса³⁵, I.N. Aleksandrov⁷⁷, C. Alexa^{27b}, T. Alexopoulos¹⁰, M. Althroob¹²⁴, B. Ali¹³⁸, G. Alimonti^{66a}, J. Alison³⁶, S.P. Alkire¹⁴⁵, C. Allaire¹²⁸, B.M.M. Allbrooke¹⁵³, B.W. Allen¹²⁷, P.P. Allport²¹, A. Aloisio^{67a,67b}, A. Alonso³⁹, F. Alonso⁸⁶, C. Alpigiani¹⁴⁵, A.A. Alshehri⁵⁵, M.I. Alstaty⁹⁹, B. Alvarez Gonzalez³⁵, D. Álvarez Piqueras¹⁷¹, M.G. Alviggi^{67a,67b}, B.T. Amadio¹⁸, Y. Amaral Coutinho^{78b}, L. Ambroz¹³¹, C. Amelung²⁶, D. Amidei¹⁰³, S.P. Amor Dos Santos^{136a,136c}, S. Amoroso³⁵, C.S. Amrouche⁵², C. Anastopoulos¹⁴⁶, L.S. Ancu⁵², N. Andari²¹, T. Andeen¹¹, C.F. Anders^{59b}, J.K. Anders²⁰, K.J. Anderson³⁶, A. Andreazza^{66a,66b}, V. Andrei^{59a}, C.R. Anelli¹⁷³, S. Angelidakis³⁷, I. Angelozzi¹¹⁸, A. Angerami³⁸, A.V. Anisenkov^{120b,120a}, A. Annovi^{69a}, C. Antel^{59a}, M.T. Anthony¹⁴⁶, M. Antonelli⁴⁹, D.J.A. Antrim¹⁶⁸, F. Anulli^{70a}, M. Aoki⁷⁹, L. Aperio Bella³⁵, G. Arabidze¹⁰⁴, Y. Arai⁷⁹, J.P. Araque^{136a}, V. Araujo Ferraz^{78b}, R. Araujo Pereira^{78b}, A.T.H. Arce⁴⁷, R.E. Ardell⁹¹, F.A. Arduh⁸⁶, J.-F. Arguin¹⁰⁷, S. Argyropoulos⁷⁵, A.J. Armbruster³⁵, L.J. Armitage⁹⁰, A. Armstrong¹⁶⁸, O. Arnaez¹⁶⁴, H. Arnold¹¹⁸, M. Arratia³¹, O. Arslan²⁴, A. Artamonov^{109,*}, G. Artoni¹³¹, S. Artz⁹⁷, S. Asai¹⁶⁰, N. Asbah⁴⁴, A. Ashkenazi¹⁵⁸, E.M. Asimakopoulou¹⁶⁹, L. Asquith¹⁵³, K. Assamagan²⁹, R. Astalos^{28a}, R.J. Atkin^{32a}, M. Atkinson¹⁷⁰, N.B. Atlay¹⁴⁸, K. Augsten¹³⁸, G. Avolio³⁵, R. Avramidou^{58a}, B. Axen¹⁸, M.K. Ayoub^{15a}, G. Azuelos^{107,at}, A.E. Baas^{59a}, M.J. Baca²¹, H. Bachacou¹⁴², K. Bachas^{65a,65b}, M. Backes¹³¹, P. Bagnaia^{70a,70b}, M. Bahmani⁸², H. Bahrasemani¹⁴⁹, A.J. Bailey¹⁷¹, J.T. Baines¹⁴¹, M. Bajic³⁹, C. Bakalis¹⁰, O.K. Baker¹⁸⁰, P.J. Bakker¹¹⁸, D. Bakshi Gupta⁹³, E.M. Baldin^{120b,120a}, P. Balek¹⁷⁷, F. Balli¹⁴², W.K. Balunas¹³³, J. Balz⁹⁷, E. Banas⁸², A. Bandyopadhyay²⁴, S. Banerjee^{178,k}, A.A.E. Bannoura¹⁷⁹, L. Barak¹⁵⁸, W.M. Barbe³⁷, E.L. Barberio¹⁰², D. Barberis^{53b,53a}, M. Barbero⁹⁹, T. Barillari¹¹³, M.-S. Barisits³⁵, J. Barkeloo¹²⁷, T. Barklow¹⁵⁰, N. Barlow³¹, R. Barnea¹⁵⁷, S.L. Barnes^{58c}, B.M. Barnett¹⁴¹, R.M. Barnett¹⁸, Z. Barnovska-Blenessy^{58a}, A. Baroncelli^{72a}, G. Barone²⁶, A.J. Barr¹³¹, L. Barranco Navarro¹⁷¹, F. Barreiro⁹⁶, J. Barreiro Guimarães da Costa^{15a}, R. Bartoldus¹⁵⁰, A.E. Barton⁸⁷, P. Bartos^{28a}, A. Basalaev¹³⁴, A. Bassalat¹²⁸, R.L. Bates⁵⁵, S.J. Batista¹⁶⁴, S. Batlamous^{34e}, J.R. Batley³¹, M. Battaglia¹⁴³, M. Bause^{70a,70b}, F. Bauer¹⁴², K.T. Bauer¹⁶⁸, H.S. Bawa^{150,m}, J.B. Beacham¹²², M.D. Beattie⁸⁷, T. Beau¹³², P.H. Beauchemin¹⁶⁷, P. Bechtle²⁴, H.C. Beck⁵¹, H.P. Beck^{20,r}, K. Becker⁵⁰, M. Becker⁹⁷, C. Becot⁴⁴, A. Beddall^{12d}, A.J. Beddall^{12a}, V.A. Bednyakov⁷⁷, M. Bedognetti¹¹⁸, C.P. Bee¹⁵², T.A. Beermann³⁵, M. Begalli^{78b}, M. Begel²⁹, A. Behera¹⁵², J.K. Behr⁴⁴, A.S. Bell⁹², G. Bella¹⁵⁸, L. Bellagamba^{23b}, A. Bellerive³³, M. Bellomo¹⁵⁷, P. Bellos⁹, K. Belotskiy¹¹⁰, N.L. Belyaev¹¹⁰, O. Benary^{158,*}, D. Benchekroun^{34a}, M. Bender¹¹², N. Benekos¹⁰, Y. Benhammou¹⁵⁸, E. Benhar Noccioli¹⁸⁰, J. Benitez⁷⁵, D.P. Benjamin⁴⁷, M. Benoit⁵², J.R. Bensinger²⁶, S. Bentvelsen¹¹⁸, L. Beresford¹³¹, M. Beretta⁴⁹, D. Berge⁴⁴, E. Bergeaas Kuutmann¹⁶⁹, N. Berger⁵, L.J. Bergsten²⁶, J. Beringer¹⁸, S. Berlendis⁷, N.R. Bernard¹⁰⁰, G. Bernardi¹³², C. Bernius¹⁵⁰, F.U. Bernlochner²⁴, T. Berry⁹¹, P. Berta⁹⁷, C. Bertella^{15a}, G. Bertoli^{43a,43b}, I.A. Bertram⁸⁷, G.J. Besjes³⁹, O. Bessidskaia Bylund^{43a,43b}, M. Bessner⁴⁴, N. Besson¹⁴², A. Bethani⁹⁸, S. Bethke¹¹³, A. Betti²⁴, A.J. Bevan⁹⁰, J. Beyer¹¹³, R.M.B. Bianchi¹³⁵, O. Biebel¹¹², D. Biedermann¹⁹, R. Bielski⁹⁸, K. Bierwagen⁹⁷,

- N.V. Biesuz^{69a,69b}, M. Biglietti^{72a}, T.R.V. Billoud¹⁰⁷, M. Bindi⁵¹, A. Bingul^{12d}, C. Bini^{70a,70b}, S. Biondi^{23b,23a}, T. Bisanz⁵¹, J.P. Biswal¹⁵⁸, C. Bitrich⁴⁶, D.M. Bjergaard⁴⁷, J.E. Black¹⁵⁰, K.M. Black²⁵, R.E. Blair⁶, T. Blazek^{28a}, I. Bloch⁴⁴, C. Blocker²⁶, A. Blue⁵⁵, U. Blumenschein⁹⁰, Dr. Blunier^{144a}, G.J. Bobbink¹¹⁸, V.S. Bobrovnikov^{120b,120a}, S.S. Bocchetta⁹⁴, A. Bocci⁴⁷, D. Boerner¹⁷⁹, D. Bogavac¹¹², A.G. Bogdanchikov^{120b,120a}, C. Bohm^{43a}, V. Boisvert⁹¹, P. Bokan^{169,y}, T. Bold^{81a}, A.S. Boldyrev¹¹¹, A.E. Bolz^{59b}, M. Bomben¹³², M. Bona⁹⁰, J.S. Bonilla¹²⁷, M. Boonekamp¹⁴², A. Borisov¹⁴⁰, G. Borissov⁸⁷, J. Bortfeldt³⁵, D. Bortoletto¹³¹, V. Bortolotto^{71a,61b,61c,71b}, D. Boscherini^{23b}, M. Bosman¹⁴, J.D. Bossio Sola³⁰, K. Bouaouda^{34a}, J. Boudreau¹³⁵, E.V. Bouhova-Thacker⁸⁷, D. Boumediene³⁷, C. Bourdarios¹²⁸, S.K. Boutle⁵⁵, A. Boveia¹²², J. Boyd³⁵, I.R. Boyko⁷⁷, A.J. Bozson⁹¹, J. Bracinik²¹, N. Brahimi⁹⁹, A. Brandt⁸, G. Brandt¹⁷⁹, O. Brandt^{59a}, F. Braren⁴⁴, U. Bratzler¹⁶¹, B. Brau¹⁰⁰, J.E. Brau¹²⁷, W.D. Breaden Madden⁵⁵, K. Brendlinger⁴⁴, A.J. Brennan¹⁰², L. Brenner⁴⁴, R. Brenner¹⁶⁹, S. Bressler¹⁷⁷, B. Brickwedde⁹⁷, D.L. Briglin²¹, D. Britton⁵⁵, D. Britzger^{59b}, I. Brock²⁴, R. Brock¹⁰⁴, G. Brooijmans³⁸, T. Brooks⁹¹, W.K. Brooks^{144b}, E. Brost¹¹⁹, J.H. Broughton²¹, P.A. Bruckman de Renstrom⁸², D. Bruncko^{28b}, A. Bruni^{23b}, G. Bruni^{23b}, L.S. Bruni¹¹⁸, S. Bruno^{71a,71b}, B.H. Brunt³¹, M. Bruschi^{23b}, N. Bruscino¹³⁵, P. Bryant³⁶, L. Bryngemark⁴⁴, T. Buanes¹⁷, Q. Buat³⁵, P. Buchholz¹⁴⁸, A.G. Buckley⁵⁵, I.A. Budagov⁷⁷, F. Buehrer⁵⁰, M.K. Bugge¹³⁰, O. Bulekov¹¹⁰, D. Bullock⁸, T.J. Burch¹¹⁹, S. Burdin⁸⁸, C.D. Burgard¹¹⁸, A.M. Burger⁵, B. Burghgrave¹¹⁹, K. Burka⁸², S. Burke¹⁴¹, I. Burmeister⁴⁵, J.T.P. Burr¹³¹, D. Büscher⁵⁰, V. Büscher⁹⁷, E. Buschmann⁵¹, P. Bussey⁵⁵, J.M. Butler²⁵, C.M. Buttar⁵⁵, J.M. Butterworth⁹², P. Butti³⁵, W. Buttlinger³⁵, A. Buzatu¹⁵⁵, A.R. Buzykaev^{120b,120a}, G. Cabras^{23b,23a}, S. Cabrera Urbán¹⁷¹, D. Caforio¹³⁸, H. Cai¹⁷⁰, V.M.M. Cairo², O. Cakir^{4a}, N. Calace⁵², P. Calafuria¹⁸, A. Calandri⁹⁹, G. Calderini¹³², P. Calfayan⁶³, G. Callea^{40b,40a}, L.P. Caloba^{78b}, S. Calvente Lopez⁹⁶, D. Calvet³⁷, S. Calvet³⁷, T.P. Calvet¹⁵², M. Calvetti^{69a,69b}, R. Camacho Toro¹³², S. Camarda³⁵, P. Camarri^{71a,71b}, D. Cameron¹³⁰, R. Caminal Armadans¹⁰⁰, C. Camincher³⁵, S. Campana³⁵, M. Campanelli⁹², A. Camplani³⁹, A. Campoverde¹⁴⁸, V. Canale^{67a,67b}, M. Cano Bret^{58c}, J. Cantero¹²⁵, T. Cao¹⁵⁸, Y. Cao¹⁷⁰, M.D.M. Capeans Garrido³⁵, I. Caprini^{27b}, M. Caprini^{27b}, M. Capua^{40b,40a}, R.M. Carbone³⁸, R. Cardarelli^{71a}, F.C. Cardillo⁵⁰, I. Carli¹³⁹, T. Carli³⁵, G. Carlino^{67a}, B.T. Carlson¹³⁵, L. Carminati^{66a,66b}, R.M.D. Carney^{43a,43b}, S. Caron¹¹⁷, E. Carquin^{144b}, S. Carrá^{66a,66b}, G.D. Carrillo-Montoya³⁵, D. Casadei^{32b}, M.P. Casado^{14,g}, A.F. Casha¹⁶⁴, M. Casolino¹⁴, D.W. Casper¹⁶⁸, R. Castelijn¹¹⁸, F.L. Castillo¹⁷¹, V. Castillo Gimenez¹⁷¹, N.F. Castro^{136a,136e}, A. Catinaccio³⁵, J.R. Catmore¹³⁰, A. Cattai³⁵, J. Caudron²⁴, V. Cavalieri²⁹, E. Cavallaro¹⁴, D. Cavalli^{66a}, M. Cavalli-Sforza¹⁴, V. Cavasinni^{69a,69b}, E. Celebi^{12b}, F. Ceradini^{72a,72b}, L. Cerdà Alberich¹⁷¹, A.S. Cerqueira^{78a}, A. Cerri¹⁵³, L. Cerrito^{71a,71b}, F. Cerutti¹⁸, A. Cervelli^{23b,23a}, S.A. Cetin^{12b}, A. Chafaq^{34a}, D. Chakraborty¹¹⁹, S.K. Chan⁵⁷, W.S. Chan¹¹⁸, Y.L. Chan^{61a}, P. Chang¹⁷⁰, J.D. Chapman³¹, D.G. Charlton²¹, C.C. Chau³³, C.A. Chavez Barajas¹⁵³, S. Che¹²², A. Chegwidden¹⁰⁴, S. Chekanov⁶, S.V. Chekulaev^{165a}, G.A. Chelkov^{77,as}, M.A. Chelstowska³⁵, C. Chen^{58a}, C.H. Chen⁷⁶, H. Chen²⁹, J. Chen^{58a}, J. Chen³⁸, S. Chen¹³³, S.J. Chen^{15c}, X. Chen^{15b,ar}, Y. Chen⁸⁰, Y-H. Chen⁴⁴, H.C. Cheng¹⁰³, H.J. Cheng^{15d}, A. Cheplakov⁷⁷, E. Cheremushkina¹⁴⁰, R. Cherkaoui El Moursli^{34e}, E. Cheu⁷, K. Cheung⁶², L. Chevalier¹⁴², V. Chiarella⁴⁹, G. Chiarelli^{69a}, G. Chiodini^{65a}, A.S. Chisholm³⁵, A. Chitan^{27b}, I. Chiu¹⁶⁰, Y.H. Chiu¹⁷³, M.V. Chizhov⁷⁷, K. Choi⁶³, A.R. Chomont¹²⁸, S. Chouridou¹⁵⁹, Y.S. Chow¹¹⁸, V. Christodoulou⁹², M.C. Chu^{61a}, J. Chudoba¹³⁷, A.J. Chuinard¹⁰¹, J.J. Chwastowski⁸², L. Chytka¹²⁶, D. Cinca⁴⁵, V. Cindro⁸⁹, I.A. Cioară²⁴, A. Ciocio¹⁸, F. Cirotto^{67a,67b}, Z.H. Citron¹⁷⁷, M. Citterio^{66a}, A. Clark⁵², M.R. Clark³⁸, P.J. Clark⁴⁸, C. Clement^{43a,43b}, Y. Coadou⁹⁹, M. Cobal^{64a,64c}, A. Coccaro^{53b,53a}, J. Cochran⁷⁶, A.E.C. Coimbra¹⁷⁷, L. Colasurdo¹¹⁷, B. Cole³⁸, A.P. Colijn¹¹⁸, J. Collot⁵⁶,

- P. Conde Muiño^{136a,136b}, E. Coniavitis⁵⁰, S.H. Connell^{32b}, I.A. Connelly⁹⁸, S. Constantinescu^{27b}, F. Conventi^{67a,au}, A.M. Cooper-Sarkar¹³¹, F. Cormier¹⁷², K.J.R. Cormier¹⁶⁴, M. Corradi^{70a,70b}, E.E. Corrigan⁹⁴, F. Corriveau^{101,ad}, A. Cortes-Gonzalez³⁵, M.J. Costa¹⁷¹, D. Costanzo¹⁴⁶, G. Cottin³¹, G. Cowan⁹¹, B.E. Cox⁹⁸, J. Crane⁹⁸, K. Cranmer¹²¹, S.J. Crawley⁵⁵, R.A. Creager¹³³, G. Cree³³, S. Crépé-Renaudin⁵⁶, F. Crescioli¹³², M. Cristinziani²⁴, V. Croft¹²¹, G. Crosetti^{40b,40a}, A. Cueto⁹⁶, T. Cuhadar Donszelmann¹⁴⁶, A.R. Cukierman¹⁵⁰, M. Curatolo⁴⁹, J. Cúth⁹⁷, S. Czekiera⁸², P. Czodrowski³⁵, M.J. Da Cunha Sargedas De Sousa^{58b,136b}, C. Da Via⁹⁸, W. Dabrowski^{81a}, T. Dado^{28a,y}, S. Dahbi^{34e}, T. Dai¹⁰³, F. Dallaire¹⁰⁷, C. Dallapiccola¹⁰⁰, M. Dam³⁹, G. D'amen^{23b,23a}, J. Damp⁹⁷, J.R. Dandoy¹³³, M.F. Daneri³⁰, N.P. Dang^{178,k}, N.D. Dann⁹⁸, M. Dannerger¹⁷², V. Dao³⁵, G. Darbo^{53b}, S. Darmora⁸, O. Dartsi⁵, A. Dattagupta¹²⁷, T. Daubney⁴⁴, S. D'Auria⁵⁵, W. Davey²⁴, C. David⁴⁴, T. Davidek¹³⁹, D.R. Davis⁴⁷, E. Dawe¹⁰², I. Dawson¹⁴⁶, K. De⁸, R. De Asmundis^{67a}, A. De Benedetti¹²⁴, S. De Castro^{23b,23a}, S. De Cecco^{70a,70b}, N. De Groot¹¹⁷, P. de Jong¹¹⁸, H. De la Torre¹⁰⁴, F. De Lorenzi⁷⁶, A. De Maria^{51,t}, D. De Pedis^{70a}, A. De Salvo^{70a}, U. De Sanctis^{71a,71b}, A. De Santo¹⁵³, K. De Vasconcelos Corga⁹⁹, J.B. De Vivie De Regie¹²⁸, C. Debenedetti¹⁴³, D.V. Dedovich⁷⁷, N. Dehghanian³, M. Del Gaudio^{40b,40a}, J. Del Peso⁹⁶, D. Delgove¹²⁸, F. Deliot¹⁴², C.M. Delitzsch⁷, M. Della Pietra^{67a,67b}, D. Della Volpe⁵², A. Dell'Acqua³⁵, L. Dell'Asta²⁵, M. Delmastro⁵, C. Delporte¹²⁸, P.A. Delsart⁵⁶, D.A. DeMarco¹⁶⁴, S. Demers¹⁸⁰, M. Demichev⁷⁷, S.P. Denisov¹⁴⁰, D. Denysiuk¹¹⁸, L. D'Eramo¹³², D. Derendarz⁸², J.E. Derkaoui^{34d}, F. Derue¹³², P. Dervan⁸⁸, K. Desch²⁴, C. Deterre⁴⁴, K. Dette¹⁶⁴, M.R. Devesa³⁰, P.O. Deviveiros³⁵, A. Dewhurst¹⁴¹, S. Dhaliwal²⁶, F.A. Di Bello⁵², A. Di Ciaccio^{71a,71b}, L. Di Ciaccio⁵, W.K. Di Clemente¹³³, C. Di Donato^{67a,67b}, A. Di Girolamo³⁵, B. Di Micco^{72a,72b}, R. Di Nardo³⁵, K.F. Di Petrillo⁵⁷, A. Di Simone⁵⁰, R. Di Sipio¹⁶⁴, D. Di Valentino³³, C. Diaconu⁹⁹, M. Diamond¹⁶⁴, F.A. Dias³⁹, T. Dias Do Vale^{136a}, M.A. Diaz^{144a}, J. Dickinson¹⁸, E.B. Diehl¹⁰³, J. Dietrich¹⁹, S. Díez Cornell⁴⁴, A. Dimitrievska¹⁸, J. Dingfelder²⁴, F. Dittus³⁵, F. Djama⁹⁹, T. Djobava^{156b}, J.I. Djuvsland^{59a}, M.A.B. Do Vale^{78c}, M. Dobre^{27b}, D. Dodsworth²⁶, C. Doglioni⁹⁴, J. Dolejsi¹³⁹, Z. Dolezal¹³⁹, M. Donadelli^{78d}, J. Donini³⁷, A. D'onofrio⁹⁰, M. D'Onofrio⁸⁸, J. Dopke¹⁴¹, A. Doria^{67a}, M.T. Dova⁸⁶, A.T. Doyle⁵⁵, E. Drechsler⁵¹, E. Dreyer¹⁴⁹, T. Dreyer⁵¹, M. Dris¹⁰, Y. Du^{58b}, J. Duarte-Campderros¹⁵⁸, F. Dubinin¹⁰⁸, M. Dubovsky^{28a}, A. Dubreuil⁵², E. Duchovni¹⁷⁷, G. Duckeck¹¹², A. Ducourthial¹³², O.A. Ducu^{107,x}, D. Duda¹¹³, A. Dudarev³⁵, A.C. Dudder⁹⁷, E.M. Duffield¹⁸, L. Duflot¹²⁸, M. Dührssen³⁵, C. Dülsen¹⁷⁹, M. Dumancic¹⁷⁷, A.E. Dumitriu^{27b,e}, A.K. Duncan⁵⁵, M. Dunford^{59a}, A. Duperrin⁹⁹, H. Duran Yildiz^{4a}, M. Düren⁵⁴, A. Durglishvili^{156b}, D. Duschinger⁴⁶, B. Dutta⁴⁴, D. Duvnjak¹, M. Dyndal⁴⁴, S. Dysch⁹⁸, B.S. Dziedzic⁸², C. Eckardt⁴⁴, K.M. Ecker¹¹³, R.C. Edgar¹⁰³, T. Eifert³⁵, G. Eigen¹⁷, K. Einsweiler¹⁸, T. Ekelof¹⁶⁹, M. El Kacimi^{34c}, R. El Kosseifi⁹⁹, V. Ellajosyula⁹⁹, M. Ellert¹⁶⁹, F. Ellinghaus¹⁷⁹, A.A. Elliot⁹⁰, N. Ellis³⁵, J. Elmsheuser²⁹, M. Elsing³⁵, D. Emeliyanov¹⁴¹, Y. Enari¹⁶⁰, J.S. Ennis¹⁷⁵, M.B. Epland⁴⁷, J. Erdmann⁴⁵, A. Ereditato²⁰, S. Errede¹⁷⁰, M. Escalier¹²⁸, C. Escobar¹⁷¹, B. Esposito⁴⁹, O. Estrada Pastor¹⁷¹, A.I. Etienne¹⁴², E. Etzion¹⁵⁸, H. Evans⁶³, A. Ezhilov¹³⁴, M. Ezzi^{34e}, F. Fabbri⁵⁵, L. Fabbri^{23b,23a}, V. Fabiani¹¹⁷, G. Facini⁹², R.M. Faisca Rodrigues Pereira^{136a}, R.M. Fakhruddinov¹⁴⁰, S. Falciano^{70a}, P.J. Falke⁵, S. Falke⁵, J. Faltova¹³⁹, Y. Fang^{15a}, M. Fanti^{66a,66b}, A. Farbin⁸, A. Farilla^{72a}, E.M. Farina^{68a,68b}, T. Farooque¹⁰⁴, S. Farrell¹⁸, S.M. Farrington¹⁷⁵, P. Farthouat³⁵, F. Fassi^{34e}, P. Fassnacht³⁵, D. Fassouliotis⁹, M. Facci Giannelli⁴⁸, A. Favareto^{53b,53a}, W.J. Fawcett⁵², L. Fayard¹²⁸, O.L. Fedin^{134,q}, W. Fedorko¹⁷², M. Feickert⁴¹, S. Feigl¹³⁰, L. Feligioni⁹⁹, C. Feng^{58b}, E.J. Feng³⁵, M. Feng⁴⁷, M.J. Fenton⁵⁵, A.B. Fenyuk¹⁴⁰, L. Feremenga⁸, J. Ferrando⁴⁴, A. Ferrari¹⁶⁹, P. Ferrari¹¹⁸, R. Ferrari^{68a}, D.E. Ferreira de Lima^{59b}, A. Ferrer¹⁷¹, D. Ferrere⁵², C. Ferretti¹⁰³, F. Fiedler⁹⁷, A. Filipčič⁸⁹, F. Filthaut¹¹⁷, K.D. Finelli²⁵, M.C.N. Fiolhais^{136a,136c,b}, L. Fiorini¹⁷¹,

- C. Fischer¹⁴, W.C. Fisher¹⁰⁴, N. Flaschel⁴⁴, I. Fleck¹⁴⁸, P. Fleischmann¹⁰³, R.R.M. Fletcher¹³³, T. Flick¹⁷⁹, B.M. Flierl¹¹², L.M. Flores¹³³, L.R. Flores Castillo^{61a}, N. Fomin¹⁷, G.T. Forcolin⁹⁸, A. Formica¹⁴², F.A. Förster¹⁴, A.C. Forti⁹⁸, A.G. Foster²¹, D. Fournier¹²⁸, H. Fox⁸⁷, S. Fracchia¹⁴⁶, P. Francavilla^{69a,69b}, M. Franchini^{23b,23a}, S. Franchino^{59a}, D. Francis³⁵, L. Franconi¹³⁰, M. Franklin⁵⁷, M. Frate¹⁶⁸, M. Fraternali^{68a,68b}, D. Freeborn⁹², S.M. Fressard-Batraneanu³⁵, B. Freund¹⁰⁷, W.S. Freund^{78b}, D. Froidevaux³⁵, J.A. Frost¹³¹, C. Fukunaga¹⁶¹, T. Fusayasu¹¹⁴, J. Fuster¹⁷¹, O. Gabizon¹⁵⁷, A. Gabrielli^{23b,23a}, A. Gabrielli¹⁸, G.P. Gach^{81a}, S. Gadatsch⁵², P. Gadow¹¹³, G. Gagliardi^{53b,53a}, L.G. Gagnon¹⁰⁷, C. Galea^{27b}, B. Galhardo^{136a,136c}, E.J. Gallas¹³¹, B.J. Gallop¹⁴¹, P. Gallus¹³⁸, G. Galster³⁹, R. Gamboa Goni⁹⁰, K.K. Gan¹²², S. Ganguly¹⁷⁷, Y. Gao⁸⁸, Y.S. Gao^{150,m}, C. García¹⁷¹, J.E. García Navarro¹⁷¹, J.A. García Pascual^{15a}, M. Garcia-Sciveres¹⁸, R.W. Gardner³⁶, N. Garelli¹⁵⁰, V. Garonne¹³⁰, K. Gasnikova⁴⁴, A. Gaudiello^{53b,53a}, G. Gaudio^{68a}, I.L. Gavrilenko¹⁰⁸, A. Gavrilyuk¹⁰⁹, C. Gay¹⁷², G. Gaycken²⁴, E.N. Gazis¹⁰, C.N.P. Gee¹⁴¹, J. Geisen⁵¹, M. Geisen⁹⁷, M.P. Geisler^{59a}, K. Gellerstedt^{43a,43b}, C. Gemme^{53b}, M.H. Genest⁵⁶, C. Geng¹⁰³, S. Gentile^{70a,70b}, C. Gentsos¹⁵⁹, S. George⁹¹, D. Gerbaudo¹⁴, G. Gessner⁴⁵, S. Ghasemi¹⁴⁸, M. Ghasemi Bostanabad¹⁷³, M. Ghneimat²⁴, B. Giacobbe^{23b}, S. Giagu^{70a,70b}, N. Giangiocomi^{23b,23a}, P. Giannetti^{69a}, S.M. Gibson⁹¹, M. Gignac¹⁴³, D. Gillberg³³, G. Gilles¹⁷⁹, D.M. Gingrich^{3,at}, M.P. Giordani^{64a,64c}, F.M. Giorgi^{23b}, P.F. Giraud¹⁴², P. Giromini⁵⁷, G. Giugliarelli^{64a,64c}, D. Giugni^{66a}, F. Giuli¹³¹, M. Giulini^{59b}, S. Gkaitatzis¹⁵⁹, I. Gkalias^{9,j}, E.L. Gkougkousis¹⁴, P. Gkountoumis¹⁰, L.K. Gladilin¹¹¹, C. Glasman⁹⁶, J. Glatzer¹⁴, P.C.F. Glaysher⁴⁴, A. Glazov⁴⁴, M. Goblirsch-Kolb²⁶, J. Godlewski⁸², S. Goldfarb¹⁰², T. Golling⁵², D. Golubkov¹⁴⁰, A. Gomes^{136a,136b,136d}, R. Goncalves Gama^{78a}, R. Gonçalo^{136a}, G. Gonella⁵⁰, L. Gonella²¹, A. Gongadze⁷⁷, F. Gonnella²¹, J.L. Gonski⁵⁷, S. González de la Hoz¹⁷¹, S. Gonzalez-Sevilla⁵², L. Goossens³⁵, P.A. Gorbounov¹⁰⁹, H.A. Gordon²⁹, B. Gorini³⁵, E. Gorini^{65a,65b}, A. Gorišek⁸⁹, A.T. Goshaw⁴⁷, C. Gössling⁴⁵, M.I. Gostkin⁷⁷, C.A. Gottardo²⁴, C.R. Goudet¹²⁸, D. Goujdami^{34c}, A.G. Goussiou¹⁴⁵, N. Govender^{32b,c}, C. Goy⁵, E. Gozani¹⁵⁷, I. Grabowska-Bold^{81a}, P.O.J. Gradin¹⁶⁹, E.C. Graham⁸⁸, J. Gramling¹⁶⁸, E. Gramstad¹³⁰, S. Grancagnolo¹⁹, V. Gratchev¹³⁴, P.M. Gravila^{27f}, C. Gray⁵⁵, H.M. Gray¹⁸, Z.D. Greenwood^{93,aj}, C. Grefe²⁴, K. Gregersen⁹², I.M. Gregor⁴⁴, P. Grenier¹⁵⁰, K. Grevtsov⁴⁴, J. Griffiths⁸, A.A. Grillo¹⁴³, K. Grimm¹⁵⁰, S. Grinstein^{14,z}, Ph. Gris³⁷, J.-F. Grivaz¹²⁸, S. Groh⁹⁷, E. Gross¹⁷⁷, J. Grosse-Knetter⁵¹, G.C. Grossi⁹³, Z.J. Grout⁹², C. Grud¹⁰³, A. Grummer¹¹⁶, L. Guan¹⁰³, W. Guan¹⁷⁸, J. Guenther³⁵, A. Guerguichon¹²⁸, F. Guescini^{165a}, D. Guest¹⁶⁸, R. Gugel⁵⁰, B. Gui¹²², T. Guillemin⁵, S. Guindon³⁵, U. Gul⁵⁵, C. Gumpert³⁵, J. Guo^{58c}, W. Guo¹⁰³, Y. Guo^{58a,s}, Z. Guo⁹⁹, R. Gupta⁴¹, S. Gurbuz^{12c}, G. Gustavino¹²⁴, B.J. Gutelman¹⁵⁷, P. Gutierrez¹²⁴, C. Gutschow⁹², C. Guyot¹⁴², M.P. Guzik^{81a}, C. Gwenlan¹³¹, C.B. Gwilliam⁸⁸, A. Haas¹²¹, C. Haber¹⁸, H.K. Hadavand⁸, N. Haddad^{34e}, A. Hadef^{58a}, S. Hageböck²⁴, M. Hagiwara¹⁶⁶, H. Hakobyan^{181,*}, M. Haleem¹⁷⁴, J. Haley¹²⁵, G. Halladjian¹⁰⁴, G.D. Hallewell⁹⁹, K. Hamacher¹⁷⁹, P. Hamal¹²⁶, K. Hamano¹⁷³, A. Hamilton^{32a}, G.N. Hamity¹⁴⁶, K. Han^{58a,ai}, L. Han^{58a}, S. Han^{15d}, K. Hanagaki^{79,v}, M. Hance¹⁴³, D.M. Handl¹¹², B. Haney¹³³, R. Hankache¹³², P. Hanke^{59a}, E. Hansen⁹⁴, J.B. Hansen³⁹, J.D. Hansen³⁹, M.C. Hansen²⁴, P.H. Hansen³⁹, K. Hara¹⁶⁶, A.S. Hard¹⁷⁸, T. Harenberg¹⁷⁹, S. Harkusha¹⁰⁵, P.F. Harrison¹⁷⁵, N.M. Hartmann¹¹², Y. Hasegawa¹⁴⁷, A. Hasib⁴⁸, S. Hassani¹⁴², S. Haug²⁰, R. Hauser¹⁰⁴, L. Hauswald⁴⁶, L.B. Havener³⁸, M. Havranek¹³⁸, C.M. Hawkes²¹, R.J. Hawkings³⁵, D. Hayden¹⁰⁴, C. Hayes¹⁵², C.P. Hays¹³¹, J.M. Hays⁹⁰, H.S. Hayward⁸⁸, S.J. Haywood¹⁴¹, M.P. Heath⁴⁸, V. Hedberg⁹⁴, L. Heelan⁸, S. Heer²⁴, K.K. Heidegger⁵⁰, J. Heilman³³, S. Heim⁴⁴, T. Heim¹⁸, B. Heinemann^{44,ao}, J.J. Heinrich¹¹², L. Heinrich¹²¹, C. Heinz⁵⁴, J. Hejbal¹³⁷, L. Helary³⁵, A. Held¹⁷², S. Hellesund¹³⁰, S. Hellman^{43a,43b}, C. Helsens³⁵, R.C.W. Henderson⁸⁷, Y. Heng¹⁷⁸, S. Henkelmann¹⁷², A.M. Henriques Correia³⁵, G.H. Herbert¹⁹,

- H. Herde²⁶, V. Herget¹⁷⁴, Y. Hernández Jiménez^{32c}, H. Herr⁹⁷, G. Herten⁵⁰, R. Hertenberger¹¹², L. Hervas³⁵, T.C. Herwig¹³³, G.G. Hesketh⁹², N.P. Hessey^{165a}, J.W. Hetherly⁴¹, S. Higashino⁷⁹, E. Higón-Rodriguez¹⁷¹, K. Hildebrand³⁶, E. Hill¹⁷³, J.C. Hill³¹, K.K. Hill²⁹, K.H. Hiller⁴⁴, S.J. Hillier²¹, M. Hils⁴⁶, I. Hinchliffe¹⁸, M. Hirose¹²⁹, D. Hirschbuehl¹⁷⁹, B. Hiti⁸⁹, O. Hladík¹³⁷, D.R. Hlaluku^{32c}, X. Hoard⁴⁸, J. Hobbs¹⁵², N. Hod^{165a}, M.C. Hodgkinson¹⁴⁶, A. Hoecker³⁵, M.R. Hoeferkamp¹¹⁶, F. Hoenig¹¹², D. Hohn²⁴, D. Hohov¹²⁸, T.R. Holmes³⁶, M. Holzbock¹¹², M. Homann⁴⁵, S. Honda¹⁶⁶, T. Honda⁷⁹, T.M. Hong¹³⁵, A. Höngle¹¹³, B.H. Hooberman¹⁷⁰, W.H. Hopkins¹²⁷, Y. Horii¹¹⁵, P. Horn⁴⁶, A.J. Horton¹⁴⁹, L.A. Horyn³⁶, J-Y. Hostachy⁵⁶, A. Hostiuc¹⁴⁵, S. Hou¹⁵⁵, A. Hoummada^{34a}, J. Howarth⁹⁸, J. Hoya⁸⁶, M. Hrabovsky¹²⁶, J. Hrdinka³⁵, I. Hristova¹⁹, J. Hrivnac¹²⁸, A. Hrynevich¹⁰⁶, T. Hryn'ova⁵, P.J. Hsu⁶², S.-C. Hsu¹⁴⁵, Q. Hu²⁹, S. Hu^{58c}, Y. Huang^{15a}, Z. Hubacek¹³⁸, F. Hubaut⁹⁹, M. Huebner²⁴, F. Huegging²⁴, T.B. Huffman¹³¹, E.W. Hughes³⁸, M. Huhtinen³⁵, R.F.H. Hunter³³, P. Huo¹⁵², A.M. Hupe³³, N. Huseynov^{77,af}, J. Huston¹⁰⁴, J. Huth⁵⁷, R. Hyneman¹⁰³, G. Iacobucci⁵², G. Iakovidis²⁹, I. Ibragimov¹⁴⁸, L. Iconomidou-Fayard¹²⁸, Z. Idrissi^{34e}, P. Iengo³⁵, R. Ignazzi³⁹, O. Igonkina^{118,ab}, R. Iguchi¹⁶⁰, T. Iizawa⁵², Y. Ikegami⁷⁹, M. Ikeno⁷⁹, D. Iliadis¹⁵⁹, N. Ilic¹⁵⁰, F. Iltzsche⁴⁶, G. Introzzi^{68a,68b}, M. Iodice^{72a}, K. Iordanidou³⁸, V. Ippolito^{70a,70b}, M.F. Isacson¹⁶⁹, N. Ishijima¹²⁹, M. Ishino¹⁶⁰, M. Ishitsuka¹⁶², W. Islam¹²⁵, C. Issever¹³¹, S. Istin^{12c,an}, F. Ito¹⁶⁶, J.M. Iturbe Ponce^{61a}, R. Iuppa^{73a,73b}, A. Ivina¹⁷⁷, H. Iwasaki⁷⁹, J.M. Izen⁴², V. Izzo^{67a}, S. Jabbar³, P. Jacka¹³⁷, P. Jackson¹, R.M. Jacobs²⁴, V. Jain², G. Jäkel¹⁷⁹, K.B. Jakobi⁹⁷, K. Jakobs⁵⁰, S. Jakobsen⁷⁴, T. Jakoubek¹³⁷, D.O. Jamin¹²⁵, D.K. Jana⁹³, R. Jansky⁵², J. Janssen²⁴, M. Janus⁵¹, P.A. Janus^{81a}, G. Jarlskog⁹⁴, N. Javadov^{77,af}, T. Javůrek⁵⁰, M. Javurkova⁵⁰, F. Jeanneau¹⁴², L. Jeanty¹⁸, J. Jejelava^{156a,ag}, A. Jelinskas¹⁷⁵, P. Jenni^{50,d}, J. Jeong⁴⁴, C. Jeske¹⁷⁵, S. Jézéquel⁵, H. Ji¹⁷⁸, J. Jia¹⁵², H. Jiang⁷⁶, Y. Jiang^{58a}, Z. Jiang¹⁵⁰, S. Jiggins⁵⁰, F.A. Jimenez Morales³⁷, J. Jimenez Pena¹⁷¹, S. Jin^{15c}, A. Jinaru^{27b}, O. Jinnouchi¹⁶², H. Jivan^{32c}, P. Johansson¹⁴⁶, K.A. Johns⁷, C.A. Johnson⁶³, W.J. Johnson¹⁴⁵, K. Jon-And^{43a,43b}, R.W.L. Jones⁸⁷, S.D. Jones¹⁵³, S. Jones⁷, T.J. Jones⁸⁸, J. Jongmanns^{59a}, P.M. Jorge^{136a,136b}, J. Jovicevic^{165a}, X. Ju¹⁷⁸, J.J. Junggeburth¹¹³, A. Juste Rozas^{14,z}, A. Kaczmarska⁸², M. Kado¹²⁸, H. Kagan¹²², M. Kagan¹⁵⁰, T. Kaji¹⁷⁶, E. Kajomovitz¹⁵⁷, C.W. Kalderon⁹⁴, A. Kaluza⁹⁷, S. Kama⁴¹, A. Kamenshchikov¹⁴⁰, L. Kanjur⁸⁹, Y. Kano¹⁶⁰, V.A. Kantserov¹¹⁰, J. Kanzaki⁷⁹, B. Kaplan¹²¹, L.S. Kaplan¹⁷⁸, D. Kar^{32c}, M.J. Kareem^{165b}, E. Karentzos¹⁰, S.N. Karpov⁷⁷, Z.M. Karpova⁷⁷, V. Kartvelishvili⁸⁷, A.N. Karyukhin¹⁴⁰, K. Kasahara¹⁶⁶, L. Kashif¹⁷⁸, R.D. Kass¹²², A. Kastanas¹⁵¹, Y. Kataoka¹⁶⁰, C. Kato¹⁶⁰, J. Katzy⁴⁴, K. Kawade⁸⁰, K. Kawagoe⁸⁵, T. Kawamoto¹⁶⁰, G. Kawamura⁵¹, E.F. Kay⁸⁸, V.F. Kazanin^{120b,120a}, R. Keeler¹⁷³, R. Kehoe⁴¹, J.S. Keller³³, E. Kellermann⁹⁴, J.J. Kempster²¹, J. Kendrick²¹, O. Kepka¹³⁷, S. Kersten¹⁷⁹, B.P. Kerševan⁸⁹, R.A. Keyes¹⁰¹, M. Khader¹⁷⁰, F. Khalil-Zada¹³, A. Khanov¹²⁵, A.G. Kharlamov^{120b,120a}, T. Kharlamova^{120b,120a}, A. Khodinov¹⁶³, T.J. Khoo⁵², E. Khramov⁷⁷, J. Khubua^{156b}, S. Kido⁸⁰, M. Kiehn⁵², C.R. Kilby⁹¹, S.H. Kim¹⁶⁶, Y.K. Kim³⁶, N. Kimura^{64a,64c}, O.M. Kind¹⁹, B.T. King⁸⁸, D. Kirchmeier⁴⁶, J. Kirk¹⁴¹, A.E. Kiryunin¹¹³, T. Kishimoto¹⁶⁰, D. Kisielewska^{81a}, V. Kitali⁴⁴, O. Kivernyk⁵, E. Kladiva^{28b}, T. Klapdor-Kleingrothaus⁵⁰, M.H. Klein¹⁰³, M. Klein⁸⁸, U. Klein⁸⁸, K. Kleinknecht⁹⁷, P. Klimek¹¹⁹, A. Klimentov²⁹, R. Klingenberg^{45,*}, T. Klingl²⁴, T. Klioutchnikova³⁵, F.F. Klitzner¹¹², P. Kluit¹¹⁸, S. Kluth¹¹³, E. Kneringer⁷⁴, E.B.F.G. Knoops⁹⁹, A. Knue⁵⁰, A. Kobayashi¹⁶⁰, D. Kobayashi⁸⁵, T. Kobayashi¹⁶⁰, M. Kobel⁴⁶, M. Kocian¹⁵⁰, P. Kodys¹³⁹, T. Koffas³³, E. Koffeman¹¹⁸, N.M. Köhler¹¹³, T. Koi¹⁵⁰, M. Kolb^{59b}, I. Koletsou⁵, T. Kondo⁷⁹, N. Kondrashova^{58c}, K. Köneke⁵⁰, A.C. König¹¹⁷, T. Kono⁷⁹, R. Konoplich^{121,ak}, V. Konstantinides⁹², N. Konstantinidis⁹², B. Konya⁹⁴, R. Kopeliansky⁶³, S. Koperny^{81a}, K. Korcyl⁸², K. Kordas¹⁵⁹, A. Korn⁹², I. Korolkov¹⁴, E.V. Korolkova¹⁴⁶, O. Kortner¹¹³, S. Kortner¹¹³, T. Kosek¹³⁹, V.V. Kostyukhin²⁴, A. Kotwal⁴⁷, A. Koulouris¹⁰, A. Kourkoumeli-Charalamplidi^{68a,68b},

- C. Kourkoumelis⁹, E. Kourlitis¹⁴⁶, V. Kouskoura²⁹, A.B. Kowalewska⁸², R. Kowalewski¹⁷³, T.Z. Kowalski^{81a}, C. Kozakai¹⁶⁰, W. Kozanecki¹⁴², A.S. Kozhin¹⁴⁰, V.A. Kramarenko¹¹¹, G. Kramberger⁸⁹, D. Krasnopevtsev¹¹⁰, M.W. Krasny¹³², A. Krasznahorkay³⁵, D. Krauss¹¹³, J.A. Kremer^{81a}, J. Kretzschmar⁸⁸, P. Krieger¹⁶⁴, K. Krizka¹⁸, K. Kroeninger⁴⁵, H. Kroha¹¹³, J. Kroll¹³⁷, J. Kroll¹³³, J. Krstic¹⁶, U. Kruchonak⁷⁷, H. Krüger²⁴, N. Krumnack⁷⁶, M.C. Kruse⁴⁷, T. Kubota¹⁰², S. Kuday^{4b}, J.T. Kuechler¹⁷⁹, S. Kuehn³⁵, A. Kugel^{59a}, F. Kuger¹⁷⁴, T. Kuhl⁴⁴, V. Kukhtin⁷⁷, R. Kukla⁹⁹, Y. Kulchitsky¹⁰⁵, S. Kuleshov^{144b}, Y.P. Kulinich¹⁷⁰, M. Kuna⁵⁶, T. Kunigo⁸³, A. Kupco¹³⁷, T. Kupfer⁴⁵, O. Kuprash¹⁵⁸, H. Kurashige⁸⁰, L.L. Kurchaninov^{165a}, Y.A. Kurochkin¹⁰⁵, M.G. Kurth^{15d}, E.S. Kuwertz¹⁷³, M. Kuze¹⁶², J. Kvita¹²⁶, T. Kwan¹⁰¹, A. La Rosa¹¹³, J.L. La Rosa Navarro^{78d}, L. La Rotonda^{40b,40a}, F. La Ruffa^{40b,40a}, C. Lacasta¹⁷¹, F. Lacava^{70a,70b}, J. Lacey⁴⁴, D.P.J. Lack⁹⁸, H. Lacker¹⁹, D. Lacour¹³², E. Ladygin⁷⁷, R. Lafaye⁵, B. Laforge¹³², T. Lagouri^{32c}, S. Lai⁵¹, S. Lammers⁶³, W. Lampl⁷, E. Lançon²⁹, U. Landgraf⁵⁰, M.P.J. Landon⁹⁰, M.C. Lanfermann⁵², V.S. Lang⁴⁴, J.C. Lange¹⁴, R.J. Langenberg³⁵, A.J. Lankford¹⁶⁸, F. Lanni²⁹, K. Lantzsch²⁴, A. Lanza^{68a}, A. Lapertosa^{53b,53a}, S. Laplace¹³², J.F. Laporte¹⁴², T. Lari^{66a}, F. Lasagni Manghi^{23b,23a}, M. Lassnig³⁵, T.S. Lau^{61a}, A. Laudrain¹²⁸, A.T. Law¹⁴³, P. Laycock⁸⁸, M. Lazzaroni^{66a,66b}, B. Le¹⁰², O. Le Dortz¹³², E. Le Guirriec⁹⁹, E.P. Le Quillec¹⁴², M. LeBlanc⁷, T. LeCompte⁶, F. Ledroit-Guillon⁵⁶, C.A. Lee²⁹, G.R. Lee^{144a}, L. Lee⁵⁷, S.C. Lee¹⁵⁵, B. Lefebvre¹⁰¹, M. Lefebvre¹⁷³, F. Legger¹¹², C. Leggett¹⁸, N. Lehmann¹⁷⁹, G. Lehmann Miotto³⁵, W.A. Leight⁴⁴, A. Leisos^{159,w}, M.A.L. Leite^{78d}, R. Leitner¹³⁹, D. Lellouch¹⁷⁷, B. Lemmer⁵¹, K.J.C. Leney⁹², T. Lenz²⁴, B. Lenzi³⁵, R. Leone⁷, S. Leone^{69a}, C. Leonidopoulos⁴⁸, G. Lerner¹⁵³, C. Leroy¹⁰⁷, R. Les¹⁶⁴, A.A.J. Lesage¹⁴², C.G. Lester³¹, M. Levchenko¹³⁴, J. Levêque⁵, D. Levin¹⁰³, L.J. Levinson¹⁷⁷, D. Lewis⁹⁰, B. Li¹⁰³, C-Q. Li^{58a}, H. Li^{58b}, L. Li^{58c}, Q. Li^{15d}, Q.Y. Li^{58a}, S. Li^{58d,58c}, X. Li^{58c}, Y. Li¹⁴⁸, Z. Liang^{15a}, B. Liberti^{71a}, A. Liblong¹⁶⁴, K. Lie^{61c}, S. Liem¹¹⁸, A. Limosani¹⁵⁴, C.Y. Lin³¹, K. Lin¹⁰⁴, T.H. Lin⁹⁷, R.A. Linck⁶³, B.E. Lindquist¹⁵², A.L. Lionti⁵², E. Lipeles¹³³, A. Lipniacka¹⁷, M. Lisovyi^{59b}, T.M. Liss^{170,aq}, A. Lister¹⁷², A.M. Litke¹⁴³, J.D. Little⁸, B. Liu⁷⁶, B.L. Liu⁶, H.B. Liu²⁹, H. Liu¹⁰³, J.B. Liu^{58a}, J.K.K. Liu¹³¹, K. Liu¹³², M. Liu^{58a}, P. Liu¹⁸, Y. Liu^{15a}, Y.L. Liu^{58a}, Y.W. Liu^{58a}, M. Livan^{68a,68b}, A. Lleres⁵⁶, J. Llorente Merino^{15a}, S.L. Lloyd⁹⁰, C.Y. Lo^{61b}, F. Lo Sterzo⁴¹, E.M. Lobodzinska⁴⁴, P. Loch⁷, F.K. Loebinger⁹⁸, A. Loesle⁵⁰, K.M. Loew²⁶, T. Lohse¹⁹, K. Lohwasser¹⁴⁶, M. Lokajicek¹³⁷, B.A. Long²⁵, J.D. Long¹⁷⁰, R.E. Long⁸⁷, L. Longo^{65a,65b}, K.A.Looper¹²², J.A. Lopez^{144b}, I. Lopez Paz¹⁴, A. Lopez Solis¹⁴⁶, J. Lorenz¹¹², N. Lorenzo Martinez⁵, M. Losada²², P.J. Lösel¹¹², X. Lou⁴⁴, X. Lou^{15a}, A. Lounis¹²⁸, J. Love⁶, P.A. Love⁸⁷, J.J. Lozano Bahilo¹⁷¹, H. Lu^{61a}, M. Lu^{58a}, N. Lu¹⁰³, Y.J. Lu⁶², H.J. Lubatti¹⁴⁵, C. Luci^{70a,70b}, A. Lucotte⁵⁶, C. Luedtke⁵⁰, F. Luehring⁶³, I. Luise¹³², W. Lukas⁷⁴, L. Luminari^{70a}, B. Lund-Jensen¹⁵¹, M.S. Lutz¹⁰⁰, P.M. Luzi¹³², D. Lynn²⁹, R. Lysak¹³⁷, E. Lytken⁹⁴, F. Lyu^{15a}, V. Lyubushkin⁷⁷, H. Ma²⁹, L.L. Ma^{58b}, Y. Ma^{58b}, G. Maccarrone⁴⁹, A. Macchiolo¹¹³, C.M. Macdonald¹⁴⁶, J. Machado Miguens^{133,136b}, D. Madaffari¹⁷¹, R. Madar³⁷, W.F. Mader⁴⁶, A. Madsen⁴⁴, N. Madysa⁴⁶, J. Maeda⁸⁰, K. Maekawa¹⁶⁰, S. Maeland¹⁷, T. Maeno²⁹, A.S. Maevskiy¹¹¹, V. Mager⁵⁰, C. Maidantchik^{78b}, T. Maier¹¹², A. Maio^{136a,136b,136d}, O. Majersky^{28a}, S. Majewski¹²⁷, Y. Makida⁷⁹, N. Makovec¹²⁸, B. Malaescu¹³², Pa. Malecki⁸², V.P. Maleev¹³⁴, F. Malek⁵⁶, U. Mallik⁷⁵, D. Malon⁶, C. Malone³¹, S. Maltezos¹⁰, S. Malyukov³⁵, J. Mamuzic¹⁷¹, G. Mancini⁴⁹, I. Mandic⁸⁹, J. Maneira^{136a}, L. Manhaes de Andrade Filho^{78a}, J. Manjarres Ramos⁴⁶, K.H. Mankinen⁹⁴, A. Mann¹¹², A. Manousos⁷⁴, B. Mansoulie¹⁴², J.D. Mansour^{15a}, M. Mantoani⁵¹, S. Manzoni^{66a,66b}, G. Marceca³⁰, L. March⁵², L. Marchese¹³¹, G. Marchiori¹³², M. Marcisovsky¹³⁷, C.A. Marin Tobon³⁵, M. Marjanovic³⁷, D.E. Marley¹⁰³, F. Marroquim^{78b}, Z. Marshall¹⁸, M.U.F Martensson¹⁶⁹, S. Marti-Garcia¹⁷¹, C.B. Martin¹²², T.A. Martin¹⁷⁵, V.J. Martin⁴⁸, B. Martin dit Latour¹⁷, M. Martinez^{14,z}, V.I. Martinez Outschoorn¹⁰⁰, S. Martin-Haugh¹⁴¹, V.S. Martoiu^{27b}, A.C. Martyniuk⁹²,

- A. Marzin³⁵, L. Masetti⁹⁷, T. Mashimo¹⁶⁰, R. Mashinistov¹⁰⁸, J. Masik⁹⁸,
A.L. Maslennikov^{120b,120a}, L.H. Mason¹⁰², L. Massa^{71a,71b}, P. Mastrandrea⁵,
A. Mastroberardino^{40b,40a}, T. Masubuchi¹⁶⁰, P. Mättig¹⁷⁹, J. Maurer^{27b}, B. Maček⁸⁹,
S.J. Maxfield⁸⁸, D.A. Maximov^{120b,120a}, R. Mazini¹⁵⁵, I. Maznas¹⁵⁹, S.M. Mazza¹⁴³,
N.C. Mc Fadden¹¹⁶, G. Mc Goldrick¹⁶⁴, S.P. Mc Kee¹⁰³, A. McCarn¹⁰³, T.G. McCarthy¹¹³,
L.I. McClymont⁹², E.F. McDonald¹⁰², J.A. Mcfayden³⁵, G. Mchedlidze⁵¹, M.A. McKay⁴¹,
K.D. McLean¹⁷³, S.J. McMahon¹⁴¹, P.C. McNamara¹⁰², C.J. McNicol¹⁷⁵, R.A. McPherson^{173,ad},
J.E. Mdhluli^{32c}, Z.A. Meadows¹⁰⁰, S. Meehan¹⁴⁵, T. Megy⁵⁰, S. Mehlhase¹¹², A. Mehta⁸⁸,
T. Meideck⁵⁶, B. Meirose⁴², D. Melini^{171,h}, B.R. Mellado Garcia^{32c}, J.D. Mellenthin⁵¹,
M. Melo^{28a}, F. Meloni²⁰, A. Melzer²⁴, S.B. Menary⁹⁸, E.D. Mendes Gouveia^{136a}, L. Meng⁸⁸,
X.T. Meng¹⁰³, A. Mengarelli^{23b,23a}, S. Menke¹¹³, E. Meoni^{40b,40a}, S. Mergelmeyer¹⁹,
C. Merlassino²⁰, P. Mermod⁵², L. Merola^{67a,67b}, C. Meroni^{66a}, F.S. Merritt³⁶, A. Messina^{70a,70b},
J. Metcalfe⁶, A.S. Mete¹⁶⁸, C. Meyer¹³³, J. Meyer¹⁵⁷, J-P. Meyer¹⁴², H. Meyer Zu Theenhausen^{59a},
F. Miano¹⁵³, R.P. Middleton¹⁴¹, L. Mijović⁴⁸, G. Mikenberg¹⁷⁷, M. Mikestikova¹³⁷, M. Mikuž⁸⁹,
M. Milesi¹⁰², A. Milic¹⁶⁴, D.A. Millar⁹⁰, D.W. Miller³⁶, A. Milov¹⁷⁷, D.A. Milstead^{43a,43b},
A.A. Minaenko¹⁴⁰, M. Miñano Moya¹⁷¹, I.A. Minashvili^{156b}, A.I. Mincer¹²¹, B. Mindur^{81a},
M. Mineev⁷⁷, Y. Minegishi¹⁶⁰, Y. Ming¹⁷⁸, L.M. Mir¹⁴, A. Mirto^{65a,65b}, K.P. Mistry¹³³,
T. Mitani¹⁷⁶, J. Mitrevski¹¹², V.A. Mitsou¹⁷¹, A. Miucci²⁰, P.S. Miyagawa¹⁴⁶, A. Mizukami⁷⁹,
J.U. Mjörnmark⁹⁴, T. Mkrtchyan¹⁸¹, M. Mlynarikova¹³⁹, T. Moa^{43a,43b}, K. Mochizuki¹⁰⁷,
P. Mogg⁵⁰, S. Mohapatra³⁸, S. Molander^{43a,43b}, R. Moles-Valls²⁴, M.C. Mondragon¹⁰⁴,
K. Mönig⁴⁴, J. Monk³⁹, E. Monnier⁹⁹, A. Montalbano¹⁴⁹, J. Montejo Berlingen³⁵, F. Monticelli⁸⁶,
S. Monzani^{66a}, R.W. Moore³, N. Morange¹²⁸, D. Moreno²², M. Moreno Llácer³⁵, P. Morettini^{53b},
M. Morgenstern¹¹⁸, S. Morgenstern³⁵, D. Mori¹⁴⁹, T. Mori¹⁶⁰, M. Morii⁵⁷, M. Morinaga¹⁷⁶,
V. Morisbak¹³⁰, A.K. Morley³⁵, G. Mornacchi³⁵, A.P. Morris⁹², J.D. Morris⁹⁰, L. Morvaj¹⁵²,
P. Moschovakos¹⁰, M. Mosidze^{156b}, H.J. Moss¹⁴⁶, J. Moss^{150,n}, K. Motohashi¹⁶², R. Mount¹⁵⁰,
E. Mountricha³⁵, E.J.W. Moyse¹⁰⁰, S. Muanza⁹⁹, F. Mueller¹¹³, J. Mueller¹³⁵, R.S.P. Mueller¹¹²,
D. Muenstermann⁸⁷, P. Mullen⁵⁵, G.A. Mullier²⁰, F.J. Munoz Sanchez⁹⁸, P. Murin^{28b},
W.J. Murray^{175,141}, A. Murrone^{66a,66b}, M. Muškinja⁸⁹, C. Mwewa^{32a}, A.G. Myagkov^{140,al},
J. Myers¹²⁷, M. Myska¹³⁸, B.P. Nachman¹⁸, O. Nackenhorst⁴⁵, K. Nagai¹³¹, K. Nagano⁷⁹,
Y. Nagasaka⁶⁰, K. Nagata¹⁶⁶, M. Nagel⁵⁰, E. Nagy⁹⁹, A.M. Nairz³⁵, Y. Nakahama¹¹⁵,
K. Nakamura⁷⁹, T. Nakamura¹⁶⁰, I. Nakano¹²³, H. Nanjo¹²⁹, F. Napolitano^{59a},
R.F. Naranjo Garcia⁴⁴, R. Narayan¹¹, D.I. Narrias Villar^{59a}, I. Naryshkin¹³⁴, T. Naumann⁴⁴,
G. Navarro²², R. Nayyar⁷, H.A. Neal¹⁰³, P.Y. Nechaeva¹⁰⁸, T.J. Neep¹⁴², A. Negri^{68a,68b},
M. Negrini^{23b}, S. Nektarijevic¹¹⁷, C. Nellist⁵¹, M.E. Nelson¹³¹, S. Nemecek¹³⁷, P. Nemethy¹²¹,
M. Nessi^{35,f}, M.S. Neubauer¹⁷⁰, M. Neumann¹⁷⁹, P.R. Newman²¹, T.Y. Ng^{61c}, Y.S. Ng¹⁹,
H.D.N. Nguyen⁹⁹, T. Nguyen Manh¹⁰⁷, E. Nibigira³⁷, R.B. Nickerson¹³¹, R. Nicolaïdou¹⁴²,
J. Nielsen¹⁴³, N. Nikiforou¹¹, V. Nikolaenko^{140,al}, I. Nikolic-Audit¹³², K. Nikolopoulos²¹,
P. Nilsson²⁹, Y. Ninomiya⁷⁹, A. Nisati^{70a}, N. Nishu^{58c}, R. Nisius¹¹³, I. Nitsche⁴⁵, T. Nitta¹⁷⁶,
T. Nobe¹⁶⁰, Y. Noguchi⁸³, M. Nomachi¹²⁹, I. Nomidis¹³², M.A. Nomura²⁹, T. Nooney⁹⁰,
M. Nordberg³⁵, N. Norjoharuddeen¹³¹, T. Novak⁸⁹, O. Novgorodova⁴⁶, R. Novotny¹³⁸,
M. Nozaki⁷⁹, L. Nozka¹²⁶, K. Ntekas¹⁶⁸, E. Nurse⁹², F. Nuti¹⁰², F.G. Oakham^{33,at},
H. Oberlack¹¹³, T. Obermann²⁴, J. Ocariz¹³², A. Ochi⁸⁰, I. Ochoa³⁸, J.P. Ochoa-Ricoux^{144a},
K. O'Connor²⁶, S. Oda⁸⁵, S. Odaka⁷⁹, A. Oh⁹⁸, S.H. Oh⁴⁷, C.C. Ohm¹⁵¹, H. Oide^{53b,53a},
H. Okawa¹⁶⁶, Y. Okazaki⁸³, Y. Okumura¹⁶⁰, T. Okuyama⁷⁹, A. Olariu^{27b}, L.F. Oleiro Seabra^{136a},
S.A. Olivares Pino^{144a}, D. Oliveira Damazio²⁹, J.L. Oliver¹, M.J.R. Olsson³⁶, A. Olszewski⁸²,
J. Olszowska⁸², D.C. O'Neil¹⁴⁹, A. Onofre^{136a,136e}, K. Onogi¹¹⁵, P.U.E. Onyisi¹¹, H. Oppen¹³⁰,
M.J. Oreglia³⁶, Y. Oren¹⁵⁸, D. Orestano^{72a,72b}, E.C. Orgill⁹⁸, N. Orlando^{61b}, A.A. O'Rourke⁴⁴,
R.S. Orr¹⁶⁴, B. Osculati^{53b,53a,*}, V. O'Shea⁵⁵, R. Ospanov^{58a}, G. Otero y Garzon³⁰, H. Otono⁸⁵,

- M. Ouchrif^{34d}, F. Ould-Saada¹³⁰, A. Ouraou¹⁴², Q. Ouyang^{15a}, M. Owen⁵⁵, R.E. Owen²¹, V.E. Ozcan^{12c}, N. Ozturk⁸, J. Pacalt¹²⁶, H.A. Pacey³¹, K. Pachal¹⁴⁹, A. Pacheco Pages¹⁴, L. Pacheco Rodriguez¹⁴², C. Padilla Aranda¹⁴, S. Pagan Griso¹⁸, M. Paganini¹⁸⁰, G. Palacino⁶³, S. Palazzo^{40b,40a}, S. Palestini³⁵, M. Palka^{81b}, D. Pallin³⁷, I. Panagoulias¹⁰, C.E. Pandini³⁵, J.G. Panduro Vazquez⁹¹, P. Pani³⁵, G. Panizzo^{64a,64c}, L. Paolozzi⁵², T.D. Papadopoulou¹⁰, K. Papageorgiou^{9,j}, A. Paramonov⁶, D. Paredes Hernandez^{61b}, S.R. Paredes Saenz¹³¹, B. Parida^{58c}, A.J. Parker⁸⁷, K.A. Parker⁴⁴, M.A. Parker³¹, F. Parodi^{53b,53a}, J.A. Parsons³⁸, U. Parzefall⁵⁰, V.R. Pascuzzi¹⁶⁴, J.M.P. Pasner¹⁴³, E. Pasqualucci^{70a}, S. Passaggio^{53b}, F. Pastore⁹¹, P. Pasuwan^{43a,43b}, S. Pataraia⁹⁷, J.R. Pater⁹⁸, A. Pathak^{178,k}, T. Pauly³⁵, B. Pearson¹¹³, M. Pedersen¹³⁰, L. Pedraza Diaz¹¹⁷, S. Pedraza Lopez¹⁷¹, R. Pedro^{136a,136b}, S.V. Peleganchuk^{120b,120a}, O. Penc¹³⁷, C. Peng^{15d}, H. Peng^{58a}, B.S. Peralva^{78a}, M.M. Perego¹⁴², A.P. Pereira Peixoto^{136a}, D.V. Perepelitsa²⁹, F. Peri¹⁹, L. Perini^{66a,66b}, H. Pernegger³⁵, S. Perrella^{67a,67b}, V.D. Peshekhonov^{77,*}, K. Peters⁴⁴, R.F.Y. Peters⁹⁸, B.A. Petersen³⁵, T.C. Petersen³⁹, E. Petit⁵⁶, A. Petridis¹, C. Petridou¹⁵⁹, P. Petroff¹²⁸, E. Petrolo^{70a}, M. Petrov¹³¹, F. Petrucci^{72a,72b}, M. Pettee¹⁸⁰, N.E. Pettersson¹⁰⁰, A. Peyaud¹⁴², R. Pezoa^{144b}, T. Pham¹⁰², F.H. Phillips¹⁰⁴, P.W. Phillips¹⁴¹, G. Piacquadio¹⁵², E. Pianori¹⁸, A. Picazio¹⁰⁰, M.A. Pickering¹³¹, R. Piegaia³⁰, J.E. Pilcher³⁶, A.D. Pilkington⁹⁸, M. Pinamonti^{71a,71b}, J.L. Pinfold³, M. Pitt¹⁷⁷, M-A. Pleier²⁹, V. Pleskot¹³⁹, E. Plotnikova⁷⁷, D. Pluth⁷⁶, P. Podberezko^{120b,120a}, R. Poettgen⁹⁴, R. Poggi⁵², L. Poggioli¹²⁸, I. Pogrebnyak¹⁰⁴, D. Pohl²⁴, I. Pokharel⁵¹, G. Polesello^{68a}, A. Poley⁴⁴, A. Pollicchio^{40b,40a}, R. Polifka³⁵, A. Polini^{23b}, C.S. Pollard⁴⁴, V. Polychronakos²⁹, D. Ponomarenko¹¹⁰, L. Pontecorvo^{70a}, G.A. Popeneiciu^{27d}, D.M. Portillo Quintero¹³², S. Pospisil¹³⁸, K. Potamianos⁴⁴, I.N. Potrap⁷⁷, C.J. Potter³¹, H. Potti¹¹, T. Poulsen⁹⁴, J. Poveda³⁵, T.D. Powell¹⁴⁶, M.E. Pozo Astigarraga³⁵, P. Pralavorio⁹⁹, S. Prell⁷⁶, D. Price⁹⁸, M. Primavera^{65a}, S. Prince¹⁰¹, N. Proklova¹¹⁰, K. Prokofiev^{61c}, F. Prokoshin^{144b}, S. Protopopescu²⁹, J. Proudfoot⁶, M. Przybycien^{81a}, A. Puri¹⁷⁰, P. Puzo¹²⁸, J. Qian¹⁰³, Y. Qin⁹⁸, A. Quadt⁵¹, M. Queitsch-Maitland⁴⁴, A. Qureshi¹, P. Rados¹⁰², F. Ragusa^{66a,66b}, G. Rahal⁹⁵, J.A. Raine⁹⁸, S. Rajagopalan²⁹, A. Ramirez Morales⁹⁰, T. Rashid¹²⁸, S. Raspovov⁵, M.G. Ratti^{66a,66b}, D.M. Rauch⁴⁴, F. Rauscher¹¹², S. Rave⁹⁷, B. Ravina¹⁴⁶, I. Ravinovich¹⁷⁷, J.H. Rawling⁹⁸, M. Raymond³⁵, A.L. Read¹³⁰, N.P. Readioff⁵⁶, M. Reale^{65a,65b}, D.M. Rebuzzi^{68a,68b}, A. Redelbach¹⁷⁴, G. Redlinger²⁹, R. Reece¹⁴³, R.G. Reed^{32c}, K. Reeves⁴², L. Rehnisch¹⁹, J. Reichert¹³³, A. Reiss⁹⁷, C. Rembser³⁵, H. Ren^{15d}, M. Rescigno^{70a}, S. Resconi^{66a}, E.D. Ressegue¹³³, S. Rettie¹⁷², E. Reynolds²¹, O.L. Rezanova^{120b,120a}, P. Reznicek¹³⁹, R. Richter¹¹³, S. Richter⁹², E. Richter-Was^{81b}, O. Ricken²⁴, M. Ridel¹³², P. Rieck¹¹³, C.J. Riegel¹⁷⁹, O. Rifki⁴⁴, M. Rijssenbeek¹⁵², A. Rimoldi^{68a,68b}, M. Rimoldi²⁰, L. Rinaldi^{23b}, G. Ripellino¹⁵¹, B. Ristić⁸⁷, E. Ritsch³⁵, I. Riu¹⁴, J.C. Rivera Vergara^{144a}, F. Rizatdinova¹²⁵, E. Rizvi⁹⁰, C. Rizzi¹⁴, R.T. Roberts⁹⁸, S.H. Robertson^{101,ad}, A. Robichaud-Veronneau¹⁰¹, D. Robinson³¹, J.E.M. Robinson⁴⁴, A. Robson⁵⁵, E. Rocco⁹⁷, C. Roda^{69a,69b}, Y. Rodina⁹⁹, S. Rodriguez Bosca¹⁷¹, A. Rodriguez Perez¹⁴, D. Rodriguez Rodriguez¹⁷¹, A.M. Rodríguez Vera^{165b}, S. Roe³⁵, C.S. Rogan⁵⁷, O. Røhne¹³⁰, R. Röhrlig¹¹³, C.P.A. Roland⁶³, J. Roloff⁵⁷, A. Romaniouk¹¹⁰, M. Romano^{23b,23a}, N. Rompotis⁸⁸, M. Ronzani¹²¹, L. Roos¹³², S. Rosati^{70a}, K. Rosbach⁵⁰, P. Rose¹⁴³, N-A. Rosien⁵¹, E. Rossi^{67a,67b}, L.P. Rossi^{53b}, L. Rossini^{66a,66b}, J.H.N. Rosten³¹, R. Rosten¹⁴, M. Rotaru^{27b}, J. Rothberg¹⁴⁵, D. Rousseau¹²⁸, D. Roy^{32c}, A. Rozanov⁹⁹, Y. Rozen¹⁵⁷, X. Ruan^{32c}, F. Rubbo¹⁵⁰, F. Rühr⁵⁰, A. Ruiz-Martinez³³, Z. Rurikova⁵⁰, N.A. Rusakovich⁷⁷, H.L. Russell¹⁰¹, J.P. Rutherford⁷, N. Ruthmann³⁵, E.M. Rüttinger^{44,1}, Y.F. Ryabov¹³⁴, M. Rybar¹⁷⁰, G. Rybkin¹²⁸, S. Ryu⁶, A. Ryzhov¹⁴⁰, G.F. Rzechorz⁵¹, P. Sabatini⁵¹, G. Sabato¹¹⁸, S. Sacerdoti¹²⁸, H.-F.-W. Sadrozinski¹⁴³, R. Sadykov⁷⁷, F. Safai Tehrani^{70a}, P. Saha¹¹⁹, M. Sahinsoy^{59a}, A. Sahu¹⁷⁹, M. Saimpert⁴⁴, M. Saito¹⁶⁰, T. Saito¹⁶⁰, H. Sakamoto¹⁶⁰, A. Sakharov^{121,ak},

- D. Salamani⁵², G. Salamanna^{72a,72b}, J.E. Salazar Loyola^{144b}, D. Salek¹¹⁸, P.H. Sales De Bruin¹⁶⁹, D. Salihagic¹¹³, A. Salnikov¹⁵⁰, J. Salt¹⁷¹, D. Salvatore^{40b,40a}, F. Salvatore¹⁵³, A. Salvucci^{61a,61b,61c}, A. Salzburger³⁵, D. Sammel⁵⁰, D. Sampsonidis¹⁵⁹, D. Sampsonidou¹⁵⁹, J. Sánchez¹⁷¹, A. Sanchez Pineda^{64a,64c}, H. Sandaker¹³⁰, C.O. Sander⁴⁴, M. Sandhoff¹⁷⁹, C. Sandoval²², D.P.C. Sankey¹⁴¹, M. Sannino^{53b,53a}, Y. Sano¹¹⁵, A. Sansoni⁴⁹, C. Santoni³⁷, H. Santos^{136a}, I. Santoyo Castillo¹⁵³, A. Sapronov⁷⁷, J.G. Saraiva^{136a,136d}, O. Sasaki⁷⁹, K. Sato¹⁶⁶, E. Sauvan⁵, P. Savard^{164,at}, N. Savic¹¹³, R. Sawada¹⁶⁰, C. Sawyer¹⁴¹, L. Sawyer^{93,aj}, C. Sbarra^{23b}, A. Sbrizzi^{23b,23a}, T. Scanlon⁹², J. Schaarschmidt¹⁴⁵, P. Schacht¹¹³, B.M. Schachtner¹¹², D. Schaefer³⁶, L. Schaefer¹³³, J. Schaeffer⁹⁷, S. Schaepe³⁵, U. Schäfer⁹⁷, A.C. Schaffer¹²⁸, D. Schaile¹¹², R.D. Schamberger¹⁵², N. Scharmberg⁹⁸, V.A. Schegelsky¹³⁴, D. Scheirich¹³⁹, F. Schenck¹⁹, M. Schernau¹⁶⁸, C. Schiavi^{53b,53a}, S. Schier¹⁴³, L.K. Schildgen²⁴, Z.M. Schillaci²⁶, E.J. Schioppa³⁵, M. Schioppa^{40b,40a}, K.E. Schleicher⁵⁰, S. Schlenker³⁵, K.R. Schmidt-Sommerfeld¹¹³, K. Schmieden³⁵, C. Schmitt⁹⁷, S. Schmitt⁴⁴, S. Schmitz⁹⁷, U. Schnoor⁵⁰, L. Schoeffel¹⁴², A. Schoening^{59b}, E. Schopf²⁴, M. Schott⁹⁷, J.F.P. Schouwenberg¹¹⁷, J. Schovancova³⁵, S. Schramm⁵², A. Schulte⁹⁷, H-C. Schultz-Coulon^{59a}, M. Schumacher⁵⁰, B.A. Schumm¹⁴³, Ph. Schune¹⁴², A. Schwartzman¹⁵⁰, T.A. Schwarz¹⁰³, H. Schweiger⁹⁸, Ph. Schwemling¹⁴², R. Schwienhorst¹⁰⁴, A. Sciandra²⁴, G. Sciolla²⁶, M. Scornajenghi^{40b,40a}, F. Scuri^{69a}, F. Scutti¹⁰², L.M. Scyboz¹¹³, J. Searcy¹⁰³, C.D. Sebastiani^{70a,70b}, P. Seema²⁴, S.C. Seidel¹¹⁶, A. Seiden¹⁴³, T. Seiss³⁶, J.M. Seixas^{78b}, G. Sekhniaidze^{67a}, K. Sekhon¹⁰³, S.J. Sekula⁴¹, N. Semprini-Cesari^{23b,23a}, S. Sen⁴⁷, S. Senkin³⁷, C. Serfon¹³⁰, L. Serin¹²⁸, L. Serkin^{64a,64b}, M. Sessa^{72a,72b}, H. Severini¹²⁴, F. Sforza¹⁶⁷, A. Sfyrla⁵², E. Shabalina⁵¹, J.D. Shahinian¹⁴³, N.W. Shaikh^{43a,43b}, L.Y. Shan^{15a}, R. Shang¹⁷⁰, J.T. Shank²⁵, M. Shapiro¹⁸, A.S. Sharma¹, A. Sharma¹³¹, P.B. Shatalov¹⁰⁹, K. Shaw¹⁵³, S.M. Shaw⁹⁸, A. Shcherbakova¹³⁴, Y. Shen¹²⁴, N. Sherafati³³, A.D. Sherman²⁵, P. Sherwood⁹², L. Shi^{155,ap}, S. Shimizu⁸⁰, C.O. Shimmin¹⁸⁰, M. Shimojima¹¹⁴, I.P.J. Shipsey¹³¹, S. Shirabe⁸⁵, M. Shiyakova⁷⁷, J. Shlomi¹⁷⁷, A. Shmeleva¹⁰⁸, D. Shoaleh Saadi¹⁰⁷, M.J. Shochet³⁶, S. Shojaii¹⁰², D.R. Shope¹²⁴, S. Shrestha¹²², E. Shulga¹¹⁰, P. Sicho¹³⁷, A.M. Sickles¹⁷⁰, P.E. Sidebo¹⁵¹, E. Sideras Haddad^{32c}, O. Sidiropoulou¹⁷⁴, A. Sidoti^{23b,23a}, F. Siegert⁴⁶, Dj. Sijacki¹⁶, J. Silva^{136a}, M. Silva Jr.¹⁷⁸, M.V. Silva Oliveira^{78a}, S.B. Silverstein^{43a}, L. Simic⁷⁷, S. Simion¹²⁸, E. Simioni⁹⁷, M. Simon⁹⁷, P. Sinervo¹⁶⁴, N.B. Sinev¹²⁷, M. Sioli^{23b,23a}, G. Siragusa¹⁷⁴, I. Siral¹⁰³, S.Yu. Sivoklokov¹¹¹, J. Sjölin^{43a,43b}, M.B. Skinner⁸⁷, P. Skubic¹²⁴, M. Slater²¹, T. Slavicek¹³⁸, M. Slawinska⁸², K. Sliwa¹⁶⁷, R. Slovák¹³⁹, V. Smakhtin¹⁷⁷, B.H. Smart⁵, J. Smiesko^{28a}, N. Smirnov¹¹⁰, S.Yu. Smirnov¹¹⁰, Y. Smirnov¹¹⁰, L.N. Smirnova¹¹¹, O. Smirnova⁹⁴, J.W. Smith⁵¹, M.N.K. Smith³⁸, R.W. Smith³⁸, M. Smizanska⁸⁷, K. Smolek¹³⁸, A.A. Snesarev¹⁰⁸, I.M. Snyder¹²⁷, S. Snyder²⁹, R. Sobie^{173,ad}, A.M. Soffa¹⁶⁸, A. Soffer¹⁵⁸, A. Søgaard⁴⁸, D.A. Soh¹⁵⁵, G. Sokhrannyi⁸⁹, C.A. Solans Sanchez³⁵, M. Solar¹³⁸, E.Yu. Soldatov¹¹⁰, U. Soldevila¹⁷¹, A.A. Solodkov¹⁴⁰, A. Soloshenko⁷⁷, O.V. Solovyanov¹⁴⁰, V. Solovyev¹³⁴, P. Sommer¹⁴⁶, H. Son¹⁶⁷, W. Song¹⁴¹, A. Sopczak¹³⁸, F. Sopkova^{28b}, D. Sosa^{59b}, C.L. Sotiropoulou^{69a,69b}, S. Sottocornola^{68a,68b}, R. Soualah^{64a,64c,i}, A.M. Soukharev^{120b,120a}, D. South⁴⁴, B.C. Sowden⁹¹, S. Spagnolo^{65a,65b}, M. Spalla¹¹³, M. Spangenberg¹⁷⁵, F. Spanò⁹¹, D. Sperlich¹⁹, F. Spettel¹¹³, T.M. Spieker^{59a}, R. Spighi^{23b}, G. Spigo³⁵, L.A. Spiller¹⁰², D.P. Spiteri⁵⁵, M. Spousta¹³⁹, A. Stabile^{66a,66b}, R. Stamen^{59a}, S. Stamm¹⁹, E. Stanecka⁸², R.W. Stanek⁶, C. Stanescu^{72a}, B. Stanislaus¹³¹, M.M. Stanitzki⁴⁴, B. Stapf¹¹⁸, S. Stapnes¹³⁰, E.A. Starchenko¹⁴⁰, G.H. Stark³⁶, J. Stark⁵⁶, S.H. Stark³⁹, P. Staroba¹³⁷, P. Starovoitov^{59a}, S. Stärz³⁵, R. Staszewski⁸², M. Stegler⁴⁴, P. Steinberg²⁹, B. Stelzer¹⁴⁹, H.J. Stelzer³⁵, O. Stelzer-Chilton^{165a}, H. Stenzel⁵⁴, T.J. Stevenson⁹⁰, G.A. Stewart⁵⁵, M.C. Stockton¹²⁷, G. Stoica^{27p}, P. Stolte⁵¹, S. Stonjek¹¹³, A. Straessner⁴⁶, J. Strandberg¹⁵¹, S. Strandberg^{43a,43b}, M. Strauss¹²⁴, P. Strizenec^{28b}, R. Ströhmer¹⁷⁴, D.M. Strom¹²⁷, R. Stroynowski⁴¹, A. Strubig⁴⁸, S.A. Stucci²⁹, B. Stugu¹⁷, J. Stupak¹²⁴,

- N.A. Styles⁴⁴, D. Su¹⁵⁰, J. Su¹³⁵, S. Suchek^{59a}, Y. Sugaya¹²⁹, M. Suk¹³⁸, V.V. Sulin¹⁰⁸, D.M.S. Sultan⁵², S. Sultansoy^{4c}, T. Sumida⁸³, S. Sun¹⁰³, X. Sun³, K. Suruliz¹⁵³, C.J.E. Suster¹⁵⁴, M.R. Sutton¹⁵³, S. Suzuki⁷⁹, M. Svatos¹³⁷, M. Swiatlowski³⁶, S.P. Swift², A. Sydorenko⁹⁷, I. Sykora^{28a}, T. Sykora¹³⁹, D. Ta⁹⁷, K. Tackmann^{44,aa}, J. Taenzer¹⁵⁸, A. Taffard¹⁶⁸, R. Tafirout^{165a}, E. Tahirovic⁹⁰, N. Taiblum¹⁵⁸, H. Takai²⁹, R. Takashima⁸⁴, E.H. Takasugi¹¹³, K. Takeda⁸⁰, T. Takeshita¹⁴⁷, Y. Takubo⁷⁹, M. Talby⁹⁹, A.A. Talyshев^{120b,120a}, J. Tanaka¹⁶⁰, M. Tanaka¹⁶², R. Tanaka¹²⁸, R. Tanioka⁸⁰, B.B. Tannenwald¹²², S. Tapia Araya^{144b}, S. Tapprogge⁹⁷, A. Tarek Abouelfadl Mohamed¹³², S. Tarem¹⁵⁷, G. Tarna^{27b,e}, G.F. Tartarelli^{66a}, P. Tas¹³⁹, M. Tasevsky¹³⁷, T. Tashiro⁸³, E. Tassi^{40b,40a}, A. Tavares Delgado^{136a,136b}, Y. Tayalati^{34e}, A.C. Taylor¹¹⁶, A.J. Taylor⁴⁸, G.N. Taylor¹⁰², P.T.E. Taylor¹⁰², W. Taylor^{165b}, A.S. Tee⁸⁷, P. Teixeira-Dias⁹¹, H. Ten Kate³⁵, P.K. Teng¹⁵⁵, J.J. Teoh¹²⁹, F. Tepel¹⁷⁹, S. Terada⁷⁹, K. Terashi¹⁶⁰, J. Terron⁹⁶, S. Terzo¹⁴, M. Testa⁴⁹, R.J. Teuscher^{164,ad}, S.J. Thais¹⁸⁰, T. Theveneaux-Pelzer⁴⁴, F. Thiele³⁹, J.P. Thomas²¹, A.S. Thompson⁵⁵, P.D. Thompson²¹, L.A. Thomesen¹⁸⁰, E. Thomson¹³³, Y. Tian³⁸, R.E. Ticse Torres⁵¹, V.O. Tikhomirov^{108,am}, Yu.A. Tikhonov^{120b,120a}, S. Timoshenko¹¹⁰, P. Tipton¹⁸⁰, S. Tisserant⁹⁹, K. Todome¹⁶², S. Todorova-Nova⁵, S. Todt⁴⁶, J. Tojo⁸⁵, S. Tokár^{28a}, K. Tokushuku⁷⁹, E. Tolley¹²², K.G. Tomiwa^{32c}, M. Tomoto¹¹⁵, L. Tompkins¹⁵⁰, K. Toms¹¹⁶, B. Tong⁵⁷, P. Tornambe⁵⁰, E. Torrence¹²⁷, H. Torres⁴⁶, E. Torró Pastor¹⁴⁵, C. Tosciri¹³¹, J. Toth^{99,ac}, F. Touchard⁹⁹, D.R. Tovey¹⁴⁶, C.J. Treado¹²¹, T. Trefzger¹⁷⁴, F. Tresoldi¹⁵³, A. Tricoli²⁹, I.M. Trigger^{165a}, S. Trincaz-Duvoud¹³², M.F. Tripiana¹⁴, W. Trischuk¹⁶⁴, B. Trocmé⁵⁶, A. Trofymov¹²⁸, C. Troncon^{66a}, M. Trovatelli¹⁷³, F. Trovato¹⁵³, L. Truong^{32b}, M. Trzebinski⁸², A. Trzupek⁸², F. Tsai⁴⁴, J.C-L. Tseng¹³¹, P.V. Tsiareshka¹⁰⁵, N. Tsirintanis⁹, V. Tsiskaridze¹⁵², E.G. Tskhadadze^{156a}, I.I. Tsukerman¹⁰⁹, V. Tsulaia¹⁸, S. Tsuno⁷⁹, D. Tsybychev¹⁵², Y. Tu^{61b}, A. Tudorache^{27b}, V. Tudorache^{27b}, T.T. Tulbure^{27a}, A.N. Tuna⁵⁷, S. Turchikhin⁷⁷, D. Turgeman¹⁷⁷, I. Turk Cakir^{4b,u}, R. Turra^{66a}, P.M. Tuts³⁸, E. Tzovara⁹⁷, G. Ucchielli^{23b,23a}, I. Ueda⁷⁹, M. Ughetto^{43a,43b}, F. Ukegawa¹⁶⁶, G. Unal³⁵, A. Undrus²⁹, G. Unel¹⁶⁸, F.C. Ungaro¹⁰², Y. Unno⁷⁹, K. Uno¹⁶⁰, J. Urban^{28b}, P. Urquijo¹⁰², P. Urrejola⁹⁷, G. Usai⁸, J. Usui⁷⁹, L. Vacavant⁹⁹, V. Vacek¹³⁸, B. Vachon¹⁰¹, K.O.H. Vadla¹³⁰, A. Vaidya⁹², C. Valderanis¹¹², E. Valdes Santurio^{43a,43b}, M. Valente⁵², S. Valentinetto^{23b,23a}, A. Valero¹⁷¹, L. Valéry⁴⁴, R.A. Vallance²¹, A. Vallier⁵, J.A. Valls Ferrer¹⁷¹, T.R. Van Daalen¹⁴, W. Van Den Wollenberg¹¹⁸, H. Van der Graaf¹¹⁸, P. Van Gemmeren⁶, J. Van Nieuwkoop¹⁴⁹, I. Van Vulpen¹¹⁸, M.C. van Woerden¹¹⁸, M. Vanadia^{71a,71b}, W. Vandelli³⁵, A. Vaniachine¹⁶³, P. Vankov¹¹⁸, R. Vari^{70a}, E.W. Varnes⁷, C. Varni^{53b,53a}, T. Varol⁴¹, D. Varouchas¹²⁸, A. Vartapetian⁸, K.E. Varvell¹⁵⁴, G.A. Vasquez^{144b}, J.G. Vasquez¹⁸⁰, F. Vazeille³⁷, D. Vazquez Furelos¹⁴, T. Vazquez Schroeder¹⁰¹, J. Veatch⁵¹, V. Vecchio^{72a,72b}, L.M. Veloce¹⁶⁴, F. Veloso^{136a,136c}, S. Veneziano^{70a}, A. Ventura^{65a,65b}, M. Venturi¹⁷³, N. Venturi³⁵, V. Vercesi^{68a}, M. Verducci^{72a,72b}, C.M. Vergel Infante⁷⁶, W. Verkerke¹¹⁸, A.T. Vermeulen¹¹⁸, J.C. Vermeulen¹¹⁸, M.C. Vetterli^{149,at}, N. Viaux Maira^{144b}, O. Viazlo⁹⁴, I. Vichou^{170,*}, T. Vickey¹⁴⁶, O.E. Vickey Boeriu¹⁴⁶, G.H.A. Viehhauser¹³¹, S. Viel¹⁸, L. Vigani¹³¹, M. Villa^{23b,23a}, M. Villaplana Perez^{66a,66b}, E. Vilucchi⁴⁹, M.G. Vincter³³, V.B. Vinogradov⁷⁷, A. Vishwakarma⁴⁴, C. Vittori^{23b,23a}, I. Vivarelli¹⁵³, S. Vlachos¹⁰, M. Vogel¹⁷⁹, P. Vokac¹³⁸, G. Volpi¹⁴, S.E. Von Buddenbrock^{32c}, E. Von Toerne²⁴, V. Vorobel¹³⁹, K. Vorobev¹¹⁰, M. Vos¹⁷¹, J.H. Vossebeld⁸⁸, N. Vranjes¹⁶, M. Vranjes Milosavljevic¹⁶, V. Vrba¹³⁸, M. Vreeswijk¹¹⁸, T. Šfiligoj⁸⁹, R. Vuillermet³⁵, I. Vukotic³⁶, T. Ženiš^{28a}, L. Živković¹⁶, P. Wagner²⁴, W. Wagner¹⁷⁹, J. Wagner-Kuhr¹¹², H. Wahlberg⁸⁶, S. Wahrmund⁴⁶, K. Wakamiya⁸⁰, V.M. Walbrecht¹¹³, J. Walder⁸⁷, R. Walker¹¹², W. Walkowiak¹⁴⁸, V. Wallangen^{43a,43b}, A.M. Wang⁵⁷, C. Wang^{58b,e}, F. Wang¹⁷⁸, H. Wang¹⁸, H. Wang³, J. Wang¹⁵⁴, J. Wang^{59b}, P. Wang⁴¹, Q. Wang¹²⁴, R.-J. Wang¹³², R. Wang^{58a}, R. Wang⁶, S.M. Wang¹⁵⁵, W.T. Wang^{58a}, W. Wang^{155,p}, W.X. Wang^{58a,ae}, Y. Wang^{58a},

Z. Wang^{58c}, C. Wanotayaroj⁴⁴, A. Warburton¹⁰¹, C.P. Ward³¹, D.R. Wardrobe⁹²,
A. Washbrook⁴⁸, P.M. Watkins²¹, A.T. Watson²¹, M.F. Watson²¹, G. Watts¹⁴⁵, S. Watts⁹⁸,
B.M. Waugh⁹², A.F. Webb¹¹, S. Webb⁹⁷, C. Weber¹⁸⁰, M.S. Weber²⁰, S.A. Weber³³,
S.M. Weber^{59a}, J.S. Webster⁶, A.R. Weidberg¹³¹, B. Weinert⁶³, J. Weingarten⁵¹, M. Weirich⁹⁷,
C. Weiser⁵⁰, P.S. Wells³⁵, T. Wenaus²⁹, T. Wengler³⁵, S. Wenig³⁵, N. Wermes²⁴, M.D. Werner⁷⁶,
P. Werner³⁵, M. Wessels^{59a}, T.D. Weston²⁰, K. Whalen¹²⁷, N.L. Whallon¹⁴⁵, A.M. Wharton⁸⁷,
A.S. White¹⁰³, A. White⁸, M.J. White¹, R. White^{144b}, D. Whiteson¹⁶⁸, B.W. Whitmore⁸⁷,
F.J. Wickens¹⁴¹, W. Wiedenmann¹⁷⁸, M. Wielers¹⁴¹, C. Wiglesworth³⁹, L.A.M. Wiik-Fuchs⁵⁰,
A. Wildauer¹¹³, F. Wilk⁹⁸, H.G. Wilkens³⁵, L.J. Wilkins⁹¹, H.H. Williams¹³³, S. Williams³¹,
C. Willis¹⁰⁴, S. Willocq¹⁰⁰, J.A. Wilson²¹, I. Wingerter-Seez⁵, E. Winkels¹⁵³, F. Winkelmeier¹²⁷,
O.J. Winston¹⁵³, B.T. Winter²⁴, M. Wittgen¹⁵⁰, M. Wobisch⁹³, A. Wolf⁹⁷, T.M.H. Wolf¹¹⁸,
R. Wolff⁹⁹, M.W. Wolter⁸², H. Wolters^{136a,136c}, V.W.S. Wong¹⁷², N.L. Woods¹⁴³, S.D. Worm²¹,
B.K. Wosiek⁸², K.W. Woźniak⁸², K. Wright⁵⁵, M. Wu³⁶, S.L. Wu¹⁷⁸, X. Wu⁵², Y. Wu^{58a},
T.R. Wyatt⁹⁸, B.M. Wynne⁴⁸, S. Xella³⁹, Z. Xi¹⁰³, L. Xia¹⁷⁵, D. Xu^{15a}, H. Xu^{58a}, L. Xu²⁹,
T. Xu¹⁴², W. Xu¹⁰³, B. Yabsley¹⁵⁴, S. Yacoob^{32a}, K. Yajima¹²⁹, D.P. Yallup⁹², D. Yamaguchi¹⁶²,
Y. Yamaguchi¹⁶², A. Yamamoto⁷⁹, T. Yamanaka¹⁶⁰, F. Yamane⁸⁰, M. Yamatani¹⁶⁰,
T. Yamazaki¹⁶⁰, Y. Yamazaki⁸⁰, Z. Yan²⁵, H.J. Yang^{58c,58d}, H.T. Yang¹⁸, S. Yang⁷⁵, Y. Yang¹⁶⁰,
Z. Yang¹⁷, W-M. Yao¹⁸, Y.C. Yap⁴⁴, Y. Yasu⁷⁹, E. Yatsenko^{58c,58d}, J. Ye⁴¹, S. Ye²⁹,
I. Yeletskikh⁷⁷, E. Yigitbasi²⁵, E. Yildirim⁹⁷, K. Yorita¹⁷⁶, K. Yoshihara¹³³, C.J.S. Young³⁵,
C. Young¹⁵⁰, J. Yu⁸, J. Yu⁷⁶, X. Yue^{59a}, S.P.Y. Yuen²⁴, I. Yusuff^{31,a}, B. Zabinski⁸²,
G. Zacharis¹⁰, E. Zaffaroni⁵², R. Zaidan¹⁴, A.M. Zaitsev^{140,al}, N. Zakharchuk⁴⁴, J. Zaliecas¹⁷,
S. Zambito⁵⁷, D. Zanzi³⁵, D.R. Zaripovas⁵⁵, S.V. Zeißner⁴⁵, C. Zeitnitz¹⁷⁹, G. Zemaityte¹³¹,
J.C. Zeng¹⁷⁰, Q. Zeng¹⁵⁰, O. Zenin¹⁴⁰, D. Zerwas¹²⁸, M. Zgubič¹³¹, D.F. Zhang^{58b}, D. Zhang¹⁰³,
F. Zhang¹⁷⁸, G. Zhang^{58a,ae}, H. Zhang^{15c}, J. Zhang⁶, L. Zhang⁵⁰, L. Zhang^{58a}, M. Zhang¹⁷⁰,
P. Zhang^{15c}, R. Zhang^{58a,e}, R. Zhang²⁴, X. Zhang^{58b}, Y. Zhang^{15d}, Z. Zhang¹²⁸, X. Zhao⁴¹,
Y. Zhao^{58b,128,ai}, Z. Zhao^{58a}, A. Zhemchugov⁷⁷, B. Zhou¹⁰³, C. Zhou¹⁷⁸, L. Zhou⁴¹, M.S. Zhou^{15d},
M. Zhou¹⁵², N. Zhou^{58c}, Y. Zhou⁷, C.G. Zhu^{58b}, H.L. Zhu^{58a}, H. Zhu^{15a}, J. Zhu¹⁰³, Y. Zhu^{58a},
X. Zhuang^{15a}, K. Zhukov¹⁰⁸, V. Zhulanov^{120b,120a}, A. Zibell¹⁷⁴, D. Ziemska⁶³, N.I. Zimine⁷⁷,
S. Zimmermann⁵⁰, Z. Zinonos¹¹³, M. Zinser⁹⁷, M. Ziolkowski¹⁴⁸, G. Zobernig¹⁷⁸, A. Zoccoli^{23b,23a},
K. Zoch⁵¹, T.G. Zorbas¹⁴⁶, R. Zou³⁶, M. Zur Nedden¹⁹, L. Zwalski³⁵.

¹ Department of Physics, University of Adelaide, Adelaide; Australia

² Physics Department, SUNY Albany, Albany NY; United States of America

³ Department of Physics, University of Alberta, Edmonton AB; Canada

⁴ ^(a) Department of Physics, Ankara University, Ankara; ^(b) Istanbul Aydin University,

Istanbul; ^(c) Division of Physics, TOBB University of Economics and Technology, Ankara; Turkey

⁵ LAPP, Université Grenoble Alpes, Université Savoie Mont Blanc, CNRS/IN2P3, Annecy; France

⁶ High Energy Physics Division, Argonne National Laboratory, Argonne IL; United States of America

⁷ Department of Physics, University of Arizona, Tucson AZ; United States of America

⁸ Department of Physics, University of Texas at Arlington, Arlington TX; United States of America

⁹ Physics Department, National and Kapodistrian University of Athens, Athens; Greece

¹⁰ Physics Department, National Technical University of Athens, Zografou; Greece

¹¹ Department of Physics, University of Texas at Austin, Austin TX; United States of America

¹² ^(a) Bahçeşehir University, Faculty of Engineering and Natural Sciences, Istanbul; ^(b) Istanbul Bilgi

University, Faculty of Engineering and Natural Sciences, Istanbul; ^(c) Department of Physics,

Bogaziçi University, Istanbul; ^(d) Department of Physics Engineering, Gaziantep University,

Gaziantep; Turkey

¹³ Institute of Physics, Azerbaijan Academy of Sciences, Baku; Azerbaijan

¹⁴ Institut de Física d'Altes Energies (IFAE), Barcelona Institute of Science and Technology, Barcelona; Spain

- ¹⁵ ^(a) Institute of High Energy Physics, Chinese Academy of Sciences, Beijing; ^(b) Physics Department, Tsinghua University, Beijing; ^(c) Department of Physics, Nanjing University, Nanjing; ^(d) University of Chinese Academy of Science (UCAS), Beijing; China
- ¹⁶ Institute of Physics, University of Belgrade, Belgrade; Serbia
- ¹⁷ Department for Physics and Technology, University of Bergen, Bergen; Norway
- ¹⁸ Physics Division, Lawrence Berkeley National Laboratory and University of California, Berkeley CA; United States of America
- ¹⁹ Institut für Physik, Humboldt Universität zu Berlin, Berlin; Germany
- ²⁰ Albert Einstein Center for Fundamental Physics and Laboratory for High Energy Physics, University of Bern, Bern; Switzerland
- ²¹ School of Physics and Astronomy, University of Birmingham, Birmingham; United Kingdom
- ²² Centro de Investigaciones, Universidad Antonio Nariño, Bogota; Colombia
- ²³ ^(a) Dipartimento di Fisica e Astronomia, Università di Bologna, Bologna; ^(b) INFN Sezione di Bologna; Italy
- ²⁴ Physikalisches Institut, Universität Bonn, Bonn; Germany
- ²⁵ Department of Physics, Boston University, Boston MA; United States of America
- ²⁶ Department of Physics, Brandeis University, Waltham MA; United States of America
- ²⁷ ^(a) Transilvania University of Brasov, Brasov; ^(b) Horia Hulubei National Institute of Physics and Nuclear Engineering, Bucharest; ^(c) Department of Physics, Alexandru Ioan Cuza University of Iasi, Iasi; ^(d) National Institute for Research and Development of Isotopic and Molecular Technologies, Physics Department, Cluj-Napoca; ^(e) University Politehnica Bucharest, Bucharest; ^(f) West University in Timisoara, Timisoara; Romania
- ²⁸ ^(a) Faculty of Mathematics, Physics and Informatics, Comenius University, Bratislava; ^(b) Department of Subnuclear Physics, Institute of Experimental Physics of the Slovak Academy of Sciences, Kosice; Slovak Republic
- ²⁹ Physics Department, Brookhaven National Laboratory, Upton NY; United States of America
- ³⁰ Departamento de Física, Universidad de Buenos Aires, Buenos Aires; Argentina
- ³¹ Cavendish Laboratory, University of Cambridge, Cambridge; United Kingdom
- ³² ^(a) Department of Physics, University of Cape Town, Cape Town; ^(b) Department of Mechanical Engineering Science, University of Johannesburg, Johannesburg; ^(c) School of Physics, University of the Witwatersrand, Johannesburg; South Africa
- ³³ Department of Physics, Carleton University, Ottawa ON; Canada
- ³⁴ ^(a) Faculté des Sciences Ain Chock, Réseau Universitaire de Physique des Hautes Energies - Université Hassan II, Casablanca; ^(b) Centre National de l'Energie des Sciences Techniques Nucléaires (CNESTEN), Rabat; ^(c) Faculté des Sciences Semlalia, Université Cadi Ayyad, LPHEA-Marrakech; ^(d) Faculté des Sciences, Université Mohammed Premier and LPTPM, Oujda; ^(e) Faculté des sciences, Université Mohammed V, Rabat; Morocco
- ³⁵ CERN, Geneva; Switzerland
- ³⁶ Enrico Fermi Institute, University of Chicago, Chicago IL; United States of America
- ³⁷ LPC, Université Clermont Auvergne, CNRS/IN2P3, Clermont-Ferrand; France
- ³⁸ Nevis Laboratory, Columbia University, Irvington NY; United States of America
- ³⁹ Niels Bohr Institute, University of Copenhagen, Copenhagen; Denmark
- ⁴⁰ ^(a) Dipartimento di Fisica, Università della Calabria, Rende; ^(b) INFN Gruppo Collegato di Cosenza, Laboratori Nazionali di Frascati; Italy
- ⁴¹ Physics Department, Southern Methodist University, Dallas TX; United States of America
- ⁴² Physics Department, University of Texas at Dallas, Richardson TX; United States of America
- ⁴³ ^(a) Department of Physics, Stockholm University; ^(b) Oskar Klein Centre, Stockholm; Sweden
- ⁴⁴ Deutsches Elektronen-Synchrotron DESY, Hamburg and Zeuthen; Germany
- ⁴⁵ Lehrstuhl für Experimentelle Physik IV, Technische Universität Dortmund, Dortmund; Germany
- ⁴⁶ Institut für Kern- und Teilchenphysik, Technische Universität Dresden, Dresden; Germany
- ⁴⁷ Department of Physics, Duke University, Durham NC; United States of America
- ⁴⁸ SUPA - School of Physics and Astronomy, University of Edinburgh, Edinburgh; United Kingdom

- ⁴⁹ INFN e Laboratori Nazionali di Frascati, Frascati; Italy
⁵⁰ Physikalisches Institut, Albert-Ludwigs-Universität Freiburg, Freiburg; Germany
⁵¹ II. Physikalisches Institut, Georg-August-Universität Göttingen, Göttingen; Germany
⁵² Département de Physique Nucléaire et Corpusculaire, Université de Genève, Genève; Switzerland
⁵³ ^(a) Dipartimento di Fisica, Università di Genova, Genova; ^(b) INFN Sezione di Genova; Italy
⁵⁴ II. Physikalisches Institut, Justus-Liebig-Universität Giessen, Giessen; Germany
⁵⁵ SUPA - School of Physics and Astronomy, University of Glasgow, Glasgow; United Kingdom
⁵⁶ LPSC, Université Grenoble Alpes, CNRS/IN2P3, Grenoble INP, Grenoble; France
⁵⁷ Laboratory for Particle Physics and Cosmology, Harvard University, Cambridge MA; United States of America
⁵⁸ ^(a) Department of Modern Physics and State Key Laboratory of Particle Detection and Electronics, University of Science and Technology of China, Hefei; ^(b) Institute of Frontier and Interdisciplinary Science and Key Laboratory of Particle Physics and Particle Irradiation (MOE), Shandong University, Qingdao; ^(c) School of Physics and Astronomy, Shanghai Jiao Tong University, KLPPAC-MoE, SKLPPC, Shanghai; ^(d) Tsung-Dao Lee Institute, Shanghai; China
⁵⁹ ^(a) Kirchhoff-Institut für Physik, Ruprecht-Karls-Universität Heidelberg, Heidelberg; ^(b) Physikalisches Institut, Ruprecht-Karls-Universität Heidelberg, Heidelberg; Germany
⁶⁰ Faculty of Applied Information Science, Hiroshima Institute of Technology, Hiroshima; Japan
⁶¹ ^(a) Department of Physics, Chinese University of Hong Kong, Shatin, N.T., Hong Kong; ^(b) Department of Physics, University of Hong Kong, Hong Kong; ^(c) Department of Physics and Institute for Advanced Study, Hong Kong University of Science and Technology, Clear Water Bay, Kowloon, Hong Kong; China
⁶² Department of Physics, National Tsing Hua University, Hsinchu; Taiwan
⁶³ Department of Physics, Indiana University, Bloomington IN; United States of America
⁶⁴ ^(a) INFN Gruppo Collegato di Udine, Sezione di Trieste, Udine; ^(b) ICTP, Trieste; ^(c) Dipartimento di Chimica, Fisica e Ambiente, Università di Udine, Udine; Italy
⁶⁵ ^(a) INFN Sezione di Lecce; ^(b) Dipartimento di Matematica e Fisica, Università del Salento, Lecce; Italy
⁶⁶ ^(a) INFN Sezione di Milano; ^(b) Dipartimento di Fisica, Università di Milano, Milano; Italy
⁶⁷ ^(a) INFN Sezione di Napoli; ^(b) Dipartimento di Fisica, Università di Napoli, Napoli; Italy
⁶⁸ ^(a) INFN Sezione di Pavia; ^(b) Dipartimento di Fisica, Università di Pavia, Pavia; Italy
⁶⁹ ^(a) INFN Sezione di Pisa; ^(b) Dipartimento di Fisica E. Fermi, Università di Pisa, Pisa; Italy
⁷⁰ ^(a) INFN Sezione di Roma; ^(b) Dipartimento di Fisica, Sapienza Università di Roma, Roma; Italy
⁷¹ ^(a) INFN Sezione di Roma Tor Vergata; ^(b) Dipartimento di Fisica, Università di Roma Tor Vergata, Roma; Italy
⁷² ^(a) INFN Sezione di Roma Tre; ^(b) Dipartimento di Matematica e Fisica, Università Roma Tre, Roma; Italy
⁷³ ^(a) INFN-TIFPA; ^(b) Università degli Studi di Trento, Trento; Italy
⁷⁴ Institut für Astro- und Teilchenphysik, Leopold-Franzens-Universität, Innsbruck; Austria
⁷⁵ University of Iowa, Iowa City IA; United States of America
⁷⁶ Department of Physics and Astronomy, Iowa State University, Ames IA; United States of America
⁷⁷ Joint Institute for Nuclear Research, Dubna; Russia
⁷⁸ ^(a) Departamento de Engenharia Elétrica, Universidade Federal de Juiz de Fora (UFJF), Juiz de Fora; ^(b) Universidade Federal do Rio De Janeiro COPPE/EE/IF, Rio de Janeiro; ^(c) Universidade Federal de São João del Rei (UFSJ), São João del Rei; ^(d) Instituto de Física, Universidade de São Paulo, São Paulo; Brazil
⁷⁹ KEK, High Energy Accelerator Research Organization, Tsukuba; Japan
⁸⁰ Graduate School of Science, Kobe University, Kobe; Japan
⁸¹ ^(a) AGH University of Science and Technology, Faculty of Physics and Applied Computer Science, Krakow; ^(b) Marian Smoluchowski Institute of Physics, Jagiellonian University, Krakow; Poland
⁸² Institute of Nuclear Physics Polish Academy of Sciences, Krakow; Poland
⁸³ Faculty of Science, Kyoto University, Kyoto; Japan

- ⁸⁴ Kyoto University of Education, Kyoto; Japan
⁸⁵ Research Center for Advanced Particle Physics and Department of Physics, Kyushu University, Fukuoka ; Japan
⁸⁶ Instituto de Física La Plata, Universidad Nacional de La Plata and CONICET, La Plata; Argentina
⁸⁷ Physics Department, Lancaster University, Lancaster; United Kingdom
⁸⁸ Oliver Lodge Laboratory, University of Liverpool, Liverpool; United Kingdom
⁸⁹ Department of Experimental Particle Physics, Jožef Stefan Institute and Department of Physics, University of Ljubljana, Ljubljana; Slovenia
⁹⁰ School of Physics and Astronomy, Queen Mary University of London, London; United Kingdom
⁹¹ Department of Physics, Royal Holloway University of London, Egham; United Kingdom
⁹² Department of Physics and Astronomy, University College London, London; United Kingdom
⁹³ Louisiana Tech University, Ruston LA; United States of America
⁹⁴ Fysiska institutionen, Lunds universitet, Lund; Sweden
⁹⁵ Centre de Calcul de l'Institut National de Physique Nucléaire et de Physique des Particules (IN2P3), Villeurbanne; France
⁹⁶ Departamento de Física Teorica C-15 and CIAFF, Universidad Autónoma de Madrid, Madrid; Spain
⁹⁷ Institut für Physik, Universität Mainz, Mainz; Germany
⁹⁸ School of Physics and Astronomy, University of Manchester, Manchester; United Kingdom
⁹⁹ CPPM, Aix-Marseille Université, CNRS/IN2P3, Marseille; France
¹⁰⁰ Department of Physics, University of Massachusetts, Amherst MA; United States of America
¹⁰¹ Department of Physics, McGill University, Montreal QC; Canada
¹⁰² School of Physics, University of Melbourne, Victoria; Australia
¹⁰³ Department of Physics, University of Michigan, Ann Arbor MI; United States of America
¹⁰⁴ Department of Physics and Astronomy, Michigan State University, East Lansing MI; United States of America
¹⁰⁵ B.I. Stepanov Institute of Physics, National Academy of Sciences of Belarus, Minsk; Belarus
¹⁰⁶ Research Institute for Nuclear Problems of Byelorussian State University, Minsk; Belarus
¹⁰⁷ Group of Particle Physics, University of Montreal, Montreal QC; Canada
¹⁰⁸ P.N. Lebedev Physical Institute of the Russian Academy of Sciences, Moscow; Russia
¹⁰⁹ Institute for Theoretical and Experimental Physics (ITEP), Moscow; Russia
¹¹⁰ National Research Nuclear University MEPhI, Moscow; Russia
¹¹¹ D.V. Skobeltsyn Institute of Nuclear Physics, M.V. Lomonosov Moscow State University, Moscow; Russia
¹¹² Fakultät für Physik, Ludwig-Maximilians-Universität München, München; Germany
¹¹³ Max-Planck-Institut für Physik (Werner-Heisenberg-Institut), München; Germany
¹¹⁴ Nagasaki Institute of Applied Science, Nagasaki; Japan
¹¹⁵ Graduate School of Science and Kobayashi-Maskawa Institute, Nagoya University, Nagoya; Japan
¹¹⁶ Department of Physics and Astronomy, University of New Mexico, Albuquerque NM; United States of America
¹¹⁷ Institute for Mathematics, Astrophysics and Particle Physics, Radboud University Nijmegen/Nikhef, Nijmegen; Netherlands
¹¹⁸ Nikhef National Institute for Subatomic Physics and University of Amsterdam, Amsterdam; Netherlands
¹¹⁹ Department of Physics, Northern Illinois University, DeKalb IL; United States of America
¹²⁰ ^(a)Budker Institute of Nuclear Physics, SB RAS, Novosibirsk;^(b)Novosibirsk State University Novosibirsk; Russia
¹²¹ Department of Physics, New York University, New York NY; United States of America
¹²² Ohio State University, Columbus OH; United States of America
¹²³ Faculty of Science, Okayama University, Okayama; Japan
¹²⁴ Homer L. Dodge Department of Physics and Astronomy, University of Oklahoma, Norman OK; United States of America

- ¹²⁵ Department of Physics, Oklahoma State University, Stillwater OK; United States of America
¹²⁶ Palacký University, RCPTM, Joint Laboratory of Optics, Olomouc; Czech Republic
¹²⁷ Center for High Energy Physics, University of Oregon, Eugene OR; United States of America
¹²⁸ LAL, Université Paris-Sud, CNRS/IN2P3, Université Paris-Saclay, Orsay; France
¹²⁹ Graduate School of Science, Osaka University, Osaka; Japan
¹³⁰ Department of Physics, University of Oslo, Oslo; Norway
¹³¹ Department of Physics, Oxford University, Oxford; United Kingdom
¹³² LPNHE, Sorbonne Université, Paris Diderot Sorbonne Paris Cité, CNRS/IN2P3, Paris; France
¹³³ Department of Physics, University of Pennsylvania, Philadelphia PA; United States of America
¹³⁴ Konstantinov Nuclear Physics Institute of National Research Centre “Kurchatov Institute”, PNPI, St. Petersburg; Russia
¹³⁵ Department of Physics and Astronomy, University of Pittsburgh, Pittsburgh PA; United States of America
¹³⁶ ^(a) Laboratório de Instrumentação e Física Experimental de Partículas - LIP;^(b) Departamento de Física, Faculdade de Ciências, Universidade de Lisboa, Lisboa;^(c) Departamento de Física, Universidade de Coimbra, Coimbra;^(d) Centro de Física Nuclear da Universidade de Lisboa, Lisboa;^(e) Departamento de Física, Universidade do Minho, Braga;^(f) Departamento de Física Teórica y del Cosmos, Universidad de Granada, Granada (Spain);^(g) Dep Física and CEFITEC of Faculdade de Ciências e Tecnologia, Universidade Nova de Lisboa, Caparica; Portugal
¹³⁷ Institute of Physics, Academy of Sciences of the Czech Republic, Prague; Czech Republic
¹³⁸ Czech Technical University in Prague, Prague; Czech Republic
¹³⁹ Charles University, Faculty of Mathematics and Physics, Prague; Czech Republic
¹⁴⁰ State Research Center Institute for High Energy Physics, NRC KI, Protvino; Russia
¹⁴¹ Particle Physics Department, Rutherford Appleton Laboratory, Didcot; United Kingdom
¹⁴² IRFU, CEA, Université Paris-Saclay, Gif-sur-Yvette; France
¹⁴³ Santa Cruz Institute for Particle Physics, University of California Santa Cruz, Santa Cruz CA; United States of America
¹⁴⁴ ^(a) Departamento de Física, Pontificia Universidad Católica de Chile, Santiago;^(b) Departamento de Física, Universidad Técnica Federico Santa María, Valparaíso; Chile
¹⁴⁵ Department of Physics, University of Washington, Seattle WA; United States of America
¹⁴⁶ Department of Physics and Astronomy, University of Sheffield, Sheffield; United Kingdom
¹⁴⁷ Department of Physics, Shinshu University, Nagano; Japan
¹⁴⁸ Department Physik, Universität Siegen, Siegen; Germany
¹⁴⁹ Department of Physics, Simon Fraser University, Burnaby BC; Canada
¹⁵⁰ SLAC National Accelerator Laboratory, Stanford CA; United States of America
¹⁵¹ Physics Department, Royal Institute of Technology, Stockholm; Sweden
¹⁵² Departments of Physics and Astronomy, Stony Brook University, Stony Brook NY; United States of America
¹⁵³ Department of Physics and Astronomy, University of Sussex, Brighton; United Kingdom
¹⁵⁴ School of Physics, University of Sydney, Sydney; Australia
¹⁵⁵ Institute of Physics, Academia Sinica, Taipei; Taiwan
¹⁵⁶ ^(a) E. Andronikashvili Institute of Physics, Iv. Javakhishvili Tbilisi State University, Tbilisi;^(b) High Energy Physics Institute, Tbilisi State University, Tbilisi; Georgia
¹⁵⁷ Department of Physics, Technion, Israel Institute of Technology, Haifa; Israel
¹⁵⁸ Raymond and Beverly Sackler School of Physics and Astronomy, Tel Aviv University, Tel Aviv; Israel
¹⁵⁹ Department of Physics, Aristotle University of Thessaloniki, Thessaloniki; Greece
¹⁶⁰ International Center for Elementary Particle Physics and Department of Physics, University of Tokyo, Tokyo; Japan
¹⁶¹ Graduate School of Science and Technology, Tokyo Metropolitan University, Tokyo; Japan
¹⁶² Department of Physics, Tokyo Institute of Technology, Tokyo; Japan
¹⁶³ Tomsk State University, Tomsk; Russia

- ¹⁶⁴ Department of Physics, University of Toronto, Toronto ON; Canada
¹⁶⁵ ^(a) TRIUMF, Vancouver BC; ^(b) Department of Physics and Astronomy, York University, Toronto ON; Canada
¹⁶⁶ Division of Physics and Tomonaga Center for the History of the Universe, Faculty of Pure and Applied Sciences, University of Tsukuba, Tsukuba; Japan
¹⁶⁷ Department of Physics and Astronomy, Tufts University, Medford MA; United States of America
¹⁶⁸ Department of Physics and Astronomy, University of California Irvine, Irvine CA; United States of America
¹⁶⁹ Department of Physics and Astronomy, University of Uppsala, Uppsala; Sweden
¹⁷⁰ Department of Physics, University of Illinois, Urbana IL; United States of America
¹⁷¹ Instituto de Física Corpuscular (IFIC), Centro Mixto Universidad de Valencia - CSIC, Valencia; Spain
¹⁷² Department of Physics, University of British Columbia, Vancouver BC; Canada
¹⁷³ Department of Physics and Astronomy, University of Victoria, Victoria BC; Canada
¹⁷⁴ Fakultät für Physik und Astronomie, Julius-Maximilians-Universität Würzburg, Würzburg; Germany
¹⁷⁵ Department of Physics, University of Warwick, Coventry; United Kingdom
¹⁷⁶ Waseda University, Tokyo; Japan
¹⁷⁷ Department of Particle Physics, Weizmann Institute of Science, Rehovot; Israel
¹⁷⁸ Department of Physics, University of Wisconsin, Madison WI; United States of America
¹⁷⁹ Fakultät für Mathematik und Naturwissenschaften, Fachgruppe Physik, Bergische Universität Wuppertal, Wuppertal; Germany
¹⁸⁰ Department of Physics, Yale University, New Haven CT; United States of America
¹⁸¹ Yerevan Physics Institute, Yerevan; Armenia

^a Also at Department of Physics, University of Malaya, Kuala Lumpur; Malaysia

^b Also at Borough of Manhattan Community College, City University of New York, NY; United States of America

^c Also at Centre for High Performance Computing, CSIR Campus, Rosebank, Cape Town; South Africa

^d Also at CERN, Geneva; Switzerland

^e Also at CPPM, Aix-Marseille Université, CNRS/IN2P3, Marseille; France

^f Also at Département de Physique Nucléaire et Corpusculaire, Université de Genève, Genève; Switzerland

^g Also at Departament de Fisica de la Universitat Autònoma de Barcelona, Barcelona; Spain

^h Also at Departamento de Física Teórica y del Cosmos, Universidad de Granada, Granada (Spain); Spain

ⁱ Also at Department of Applied Physics and Astronomy, University of Sharjah, Sharjah; United Arab Emirates

^j Also at Department of Financial and Management Engineering, University of the Aegean, Chios; Greece

^k Also at Department of Physics and Astronomy, University of Louisville, Louisville, KY; United States of America

^l Also at Department of Physics and Astronomy, University of Sheffield, Sheffield; United Kingdom

^m Also at Department of Physics, California State University, Fresno CA; United States of America

ⁿ Also at Department of Physics, California State University, Sacramento CA; United States of America

^o Also at Department of Physics, King's College London, London; United Kingdom

^p Also at Department of Physics, Nanjing University, Nanjing; China

^q Also at Department of Physics, St. Petersburg State Polytechnical University, St. Petersburg; Russia

^r Also at Department of Physics, University of Fribourg, Fribourg; Switzerland

- ^s Also at Department of Physics, University of Michigan, Ann Arbor MI; United States of America
^t Also at Dipartimento di Fisica E. Fermi, Università di Pisa, Pisa; Italy
^u Also at Giresun University, Faculty of Engineering, Giresun; Turkey
^v Also at Graduate School of Science, Osaka University, Osaka; Japan
^w Also at Hellenic Open University, Patras; Greece
^x Also at Horia Hulubei National Institute of Physics and Nuclear Engineering, Bucharest; Romania
^y Also at II. Physikalisches Institut, Georg-August-Universität Göttingen, Göttingen; Germany
^z Also at Institutio Catalana de Recerca i Estudis Avancats, ICREA, Barcelona; Spain
^{aa} Also at Institut für Experimentalphysik, Universität Hamburg, Hamburg; Germany
^{ab} Also at Institute for Mathematics, Astrophysics and Particle Physics, Radboud University Nijmegen/Nikhef, Nijmegen; Netherlands
^{ac} Also at Institute for Particle and Nuclear Physics, Wigner Research Centre for Physics, Budapest; Hungary
^{ad} Also at Institute of Particle Physics (IPP); Canada
^{ae} Also at Institute of Physics, Academia Sinica, Taipei; Taiwan
^{af} Also at Institute of Physics, Azerbaijan Academy of Sciences, Baku; Azerbaijan
^{ag} Also at Institute of Theoretical Physics, Ilia State University, Tbilisi; Georgia
^{ah} Also at Istanbul University, Dept. of Physics, Istanbul; Turkey
^{ai} Also at LAL, Université Paris-Sud, CNRS/IN2P3, Université Paris-Saclay, Orsay; France
^{aj} Also at Louisiana Tech University, Ruston LA; United States of America
^{ak} Also at Manhattan College, New York NY; United States of America
^{al} Also at Moscow Institute of Physics and Technology State University, Dolgoprudny; Russia
^{am} Also at National Research Nuclear University MEPhI, Moscow; Russia
^{an} Also at Near East University, Nicosia, North Cyprus, Mersin; Turkey
^{ao} Also at Physikalisches Institut, Albert-Ludwigs-Universität Freiburg, Freiburg; Germany
^{ap} Also at School of Physics, Sun Yat-sen University, Guangzhou; China
^{aq} Also at The City College of New York, New York NY; United States of America
^{ar} Also at The Collaborative Innovation Center of Quantum Matter (CICQM), Beijing; China
^{as} Also at Tomsk State University, Tomsk, and Moscow Institute of Physics and Technology State University, Dolgoprudny; Russia
^{at} Also at TRIUMF, Vancouver BC; Canada
^{au} Also at Universita di Napoli Parthenope, Napoli; Italy
* Deceased